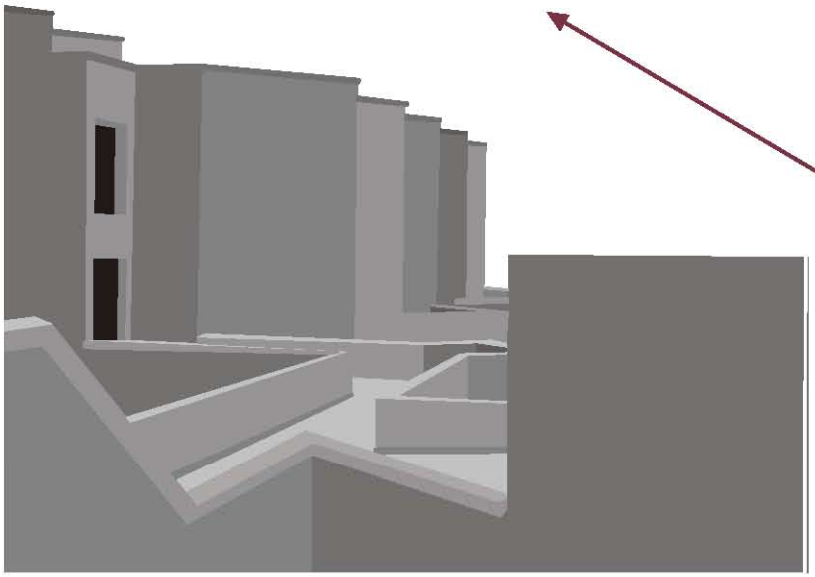

Comunicaciones del CIMAT

TOPOLOGY OPTIMIZATION BENCHMARK I.
Results for Minimum Compilance and Minimum Volume in Plane Stress Problems

Miguel A. Ochoa, S.Ivvan Valdez, Salvador Botello and Victor Cardoso

Comunicación del CIMAT No I-16-01/09-03-2016
(CC/CIMAT)

CIMAT

Topology Optimization Benchmark I. Results for minimum compliance and minimum volume in plane stress problems.

Miguel A. Ochoa, S. Ivvan Valdez, Salvador Botello and Victor Cardoso *

Centro de Investigación en Matemáticas, A.C., Departamento de Ciencias Computacionales Jalisco S/N, Col. Valenciana CP 36240 Guanajuato Gto., México

Technical report, submitted on march 8, 2016

Abstract

This article proposes a benchmark set of problems for fixed mesh topology optimization in 2 dimensions. We have established the problems based on an analysis of more than 100 articles in the specialized literature, gathering the most common dimensions, loads and fixed regions used by researchers. Most of the problems reported in specialized literature present differences in specifications such as lengths, units, materials, etcetera, by instance, some articles propose the same proportions and geometrical shape but different dimensions. Hence, the purpose of this benchmark is to unify geometrical and mechanical characteristics and load conditions, considering that the proposed problems must to be realistic, in the sense that the units are in the international system and a real-world material is used as well as load conditions. The final benchmark integrates 13 problems for plane stress using ASTM A-36 steel. Additionally, we report an approximation to the optimum solution for the compliance and volume problems (maximize stiffness with volume constraint and minimizing volume with a stress constraint respectively) using the Solid Isotropic Material with Penalization (SIMP) method and a new proposed method based on SIMP plus bisection with a Stress Constraint(SIMPSC). In-house implementations of both methods (whose are freely available for academic applications) are used.

Keywords: 2d Topology optimization, Benchmark, SIMP, stress constraint.

1 Introduction

The problem of topology optimization could be briefly described as *searching for an optimum structure in a design domain, for a given set of loads and boundary conditions, fulfilling service constraints. The optimality could depend on minimum volume, compliance or maximum rigidity, while the service constraints could be given by maximum displacements and stresses, and/or a given fraction of the initial volume.*

Despite there are many categories of topology optimization algorithms and optimization models [22],[18], most of them use the finite element method to evaluate candidate solutions, then any of these algorithms require the previous establishment of the following problem properties:

- **Design domain.** Search space dimensions and shape.
- **Boundary conditions**.Fixed displacements and load conditions:
  - **Zero displacement conditions.** Regions where the structure is fixed.
  - **Load conditions.** Regions where the structure is affected by external forces. It is necessary to establish the position and magnitude.
  - **Self body forces.** The most common is the self weight, but they could exist external forces dependent on the geometry of the body.

*e-mail:miguel.ochoa, ivvan, botello, victorc@cimat.mx

- **Material properties.** Material properties used to make the simulation: *1*)Young modulus *2*) Poisson modulus *3*)maximum permissible stress. Nevertheless the maximum permissible stress is not used for the simulation, it can be used to determine whether the material is working on the elastic range, then it must be set not only to determine if the structure is physically feasible, but also to know if the numerical simulation using elastic theory is valid.

- **Mesh.** Type, number and dimensions of elements used to mesh the domain, considering that the numerical error of the simulation depends on the mesh.

Topology optimization researchers from different groups [1, 86, 6] solve, in many cases, similar problems using different design domains, boundary conditions, material properties and meshes, which could cause the following issues:

- It is difficult to perform fair comparisons between algorithms and its implementations.

- Some articles report results using properties of materials that does not exist or without considering self weight, which is not convenient for the optimization of realistic structures.

- Using unrealistic materials and service conditions is a major concern for an adequate method, because most of the researchers ([26],[97],[86]), assume elastic properties in the material, but they do not verify if the material is actually working in the elastic range, even more, the problem formulation does not considers a constraint to verify that the candidate structure is in the elastic range neither they provide a real-world material where the elastic range is well defined.

Our proposal intend to alleviate the mentioned concerns by proposing a well defined benchmark. In this sense, other benchmark problems has been proposed, by instance, Rozvany had proposed a benchmark named: *Exact analytical solutions for some popular benchmark problems in topology optimization* [66]. In this benchmark the analytic solutions for a set of topology optimization problems is computed. Nevertheless, these problems are based in the optimization of a configuration of bars, determining positions, sizes, etc., while this article proposes a benchmark for actually optimizing the distribution of material on a domain, so, the benchmark of Rozvany is not comparable with our benchmark neither it can be used for the same kind of algorithms.

The main objective of this work is to establish a set of problems for topology optimization, detailing all the characteristics mentioned before and realistic problem configurations. By using this benchmark we can be sure that comparable algorithms are solving exactly the same problems, that the assumptions carried out by the simulations (elasticity) are true, and that the final solutions consider real-world conditions and materials, in consequence, we can perform fair comparisons among different approaches.

As a second goal of this report is to present a version of the SIMP method[68] for solving the proposed benchmark.

2 Methodology for selecting the benchmark problems

We have gathered test problems from a set of 103 articles in the specialized literature. The frequency of similar problems has been computed, grouped according the following characteristics:

- Boundary conditions. The most frequent boundary conditions considering the distance between the fixed lines/areas and loads, and loads directions.

- The geometrical shape of the search domain. That is to say, rectangular, quadrilateral, etc.

- Dimensions. The most frequent dimensions and proportions among them.

The 13 most frequent problems are significantly more used than the others, thus they where selected. Usually, their geometrical shape is exactly defined, and approximately the relative position of the loads. Most of the times, they do not define exactly the size of fixed lines (lines in a 2d view, cross-section areas of the plate), neither specify whether the loads are applied in a single point or line, in addition the thickness is not reported as well as the unit system, and the material properties are nonexistent in real-world materials. As consequence, we propose the following for circumventing the mentioned issues:

- We set the units to the standard international system, that is to say: lengths are in meters (**m**), force units are Newtons (**N**), Young modulus and yield stress is given in Pascals, and Poisson modulus is dimensionless.
- We set the sides lengths to the most frequently reported.
- We set the thickness to 1 percent of the maximum length size in order to standardize the thickness and to fulfill the hypothesis of plane stress.
- The external loads or forces are applied in a length of 10% of the length of the side they are applied in. In order to avoid numerical issues given by single-point loads.
- The material properties are set as those given by steel ASTM A-36, which possibly is the most common material used in real-life structures, and/or the most common material with similar properties than those most commonly used in industry as well as in academic problems.

3 Statistics

In Tables 1, 2, 3 and 4 the obtained data from the 103 consulted articles are condensed. The columns in tables report the following information:

- Column 1. Analyzed article. Cite to the proper article referenced at the bibliography.
- Column 2. Type test. Common problems types according to its geometrical properties they can be categorized as: Cantilever, Short Catilever, LShape, MBBB, Two Bars and Michell. Some Michell tests are marked as Michell*, this means that it is defined with two loads in boundary conditions as such showed in subfigures 2 and 3 in figure 4.
- Column 3. Load region. In Cantilever, Short Cantilever and LShape tests, the load position sometimes varies at Top, Center or Bottom of the load side as showed in figures 1, 2 and 3. In Two Bars, MBBB and Michell tests, load positions never varies as showed in figures 4, 5 and 6.
- Column 4. Load magnitude. For Michell* tests(multiload) every load is presented separated with a /.
- Columns 5, 6 an 7. Lengths of the initial domain. M, L are the side lengths, as it is shown in Figures 1,2,3,4,5 and 6. t is the thickness used, thickness cells with (v) represent volume, so these tests are in 3D.
- Column 8. Fixed regions. An * represents that the tests in the article where fixed regions at the same region that the proposed benchmark in figures 1,2,3,4,5 and 6.

A sign - indicates that there is not information about the topic in the tests at this particular article.

4 Proposed benchmark problems

In this section we provide the frequencies of the different geometries, service conditions and properties which are the basis for the benchmark proposed in this report. First, we analyze the frequency of domains dimensions and constrained lines and loads based on information gathered from papers. Using this information we proposed a benchmark problem for the 13 most common configurations.

4.1 Load magnitudes and material properties

Loads

Loaded segments have been established in Figures 1,2,3,4,5 and 6 using literals P and Q. The magnitude of the loads is defined in Table 5.

All the loads are uniformly distributed on 10% of the length of the side they are applied. The loads where set in such a way that the *Security Factor(SF)* calculated with the full domains (initial structures) is approximately *0.75*. So we are sure every structure is feasible and that a realistic load is set, that is to say that the work performed by the structure is closed its limit. SF is the value given by $SF = \frac{\sigma_{max}}{\sigma_y}$ where σ_{max} is the maximum von Mises stress in the structure, and σ_y is the yield stress which is a material property.

Reference	Test Type	Load region	Load Size	M	L	t	Hold Type
[15]	Cantilever	Central	3000	6.4	4	0.1	*
[17]	Short Cantilever	Bottom	-	250	250	-	*
	Short Cantilever	Bottom	-	20	20	20(v)	*
[61]	Cantilever	Central	-	30	10	10(v)	*
	Cantilever	Central	-	20	10	10(v)	*
	Lshape	Top	-	12	8	5(v)	
	MBBB	-	-	30	10	10(v)	
[64]	Michell	-	-	1	1	-	
	Short Cantilever	Top	-	1	1	-	
[80]	Cantilever	Central	10000	0.4	0.1	-	*
	Cantilever	Central	2000	0.08	0.02	0.02(v)	*
[89]	Cantilever	Bottom	1	100	50	-	*
	Two Bar	Central	1	80	40	-	*
	Michell*	-	1/1	50	50	-	*
[92]	MBBB	-	1	-	-	-	
	Michell	-	1	-	-	-	
[96]	-	-	-	-	-	-	
[99]	-	-	-	-	-	-	
[106]	Michell	-	1	1	1	-	*
	Short Cantilever	Bottom	1	1	1	-	*
[107]	MBBB	-	-	-	-	-	*
[1]	Cantilever	Central	1	2	1	-	
	Tshape	-	1	120	80	-	
	Michell	-	1	1	1.2	-	
	Cantilever	Central	1	5	3	2.4(v)	*
	Tshape	-	-	-	-	-(v)	*
	Lshape	Central	-	-	-	-(v)	*
	MBBB	-	-	-	-	-(v)	*
[91]	Cantilever	Central	0.5	-	-	-	*
	Cantilever	Central	1.5	-	-	-	*
[16]	Lshape	Central	1	0.6	0.4	-	*
[35]	Lshape	Central	1	0.6	0.4	-	*
[29]	Cantilever	Central	1	2	1	-	*
	Michell*	-	1/1	1	1	-	
[34]	Lshape	Top	500	0.06	0.04	-	*
	Cantilever	Central	1500	0.2	0.1	-	*
[33]	Lshape	Top	250	0.06	0.04	-	*
	Cantilever	Central	900	0.2	0.1	-	*
[41]	-	-	-	-	-	-	
[81]	Cantilever	Central	144000	1	0.25	0.1	*
	Cantilever	Central	240000	1	0.25	0.1	*
	Cantilever	Central	300000	1	0.25	0.1	*
	Cantilever	Central	500000	1	0.25	0.1	*
[74]	MBBB	-	1	-	-	-	
	Cantilever	Bottom	1	-	-	-	*
[72]	Lshape	Top	8000	0.06	0.04	-	*
[79]	Short Cantilever	Bottom	-	2	2	-	*
[88]	Cantilever	Bottom	1	20	10	-	*
[90]	MBBB	-	1	-	-	-	
	Michell	-	1	-	-	-	
[103]	Cantilever	Central	1	2	1	-	*
[95]	Short Cantilever	Bottom	1	1	1	-	*
[40]	Cantilever	Top	21000	-	-	-(v)	*
	Cantilever	Central	-	-	-	-(v)	*
	Cantilever	Bottom	-	-	-	-(v)	*
[25]	Cantilever	Central	1.2	-	-	-	*
	Cantilever	Central	1	-	-	-	*
	Cantilever	Central	0.8	-	-	-	*
[28]	Two Bar	-	1	2	1	-	*
	Lshape	Central	1	0.6	0.4	-	*
[37]	-	-	-	-	-	-	

Table 1: Statistics from topology optimization literature.

Article	**Test Type**	**Load region**	**Load Size**	M	L	t	**Hold Type**
[44]	Lshape	Top	-	-	-	-	
[49]	Two Bar	-	1	0.9	0.3	-	*
	Lshape	Top	2.5	0.6	0.4	-	*
[58]	Cantilever	Top	500	2	1	-	*
[55]	Cantilever	Central	150	40	20	-	*
[60]	Cantilever	Central	2000000	2	1	0.2	*
[62]	MBBB	-	1	3	1	-	
[67]	-	-	-	-	-	-	
[76]	Short Cantilever	Bottom	100	1	1	0.001	
	Cantilever	Central	100	1.6	1	0.001	
	Lshape	Central	100	0.6	0.4	0.001	
[78]	Cantilever	Bottom	1	2	1	-	*
	Michell	-	1	1	1	-	*
[93]	Cantilever	Central	1	0.2	0.1	-	*
	Cantilever	Bottom	1	0.15	0.1	-	*
	Cantilever	Bottom	1	0.09	0.06	0.03(v)	*
[98]	Cantilever	Central	-	4	2	-	
	MBBB	-	-	-	-	-	*
[101]	-	-	-	-	-	-	
[5]	Lshape	Top	40	1.5	1	-	*
[23]	Cantilever	Central	-	4	1	1(v)	*
	Cantilever	Central	-	2	1	-	*
	Michell*	-	-/-	2	1	-	
[77]	Cantilever	Central	1	80	40	-	*
	Cantilever	Bottom	1	80	40	-	*
[32]	Lshape	Central	-	-	-	-	*
[36]	Cantilever	Central	1	4	2	-	*
	MBBB	-	1	6	2	-	
[48]	Two Bar	Central	200	0.4	0.1	0.001	*
	Lshape	Central	20000	0.06	0.04	-	*
[50]	Cantilever	Central	1	60	30	-	*
	Michell	-	1	60	30	-	
	MBBB	-	1	90	30	-	
[57]	Cantilever	Central	-	32	16	-	*
	Cantilever	Central	-	24	12	12(v)	*
	MBBB	-	-	-	-	-	*
[94]	Lshape	Central	1	0.6	0.4	-	*
	Lshape	Top	1	0.6	0.4	-	*
	Michell	-	1	1	1	-	*
[39]	Cantilever	Central	500000	0.4	0.25	-	*
	Cantilever	Central	-	0.6	0.3	0.2(v)	*
[27]	MBBB	-	1	3	1	-	
	Cantilever	Central	1	1.5	1	-	*
	Lshape	Central	1	0.6	0.4	-	*
[105]	Michell*	-	-/-	120	120	-	*
[38]	Cantilever	Central	1	40	25	-	*
	Lshape	Top	1	20	20	-	*
	MBBB	-	1	60	20	-	
[45]	Cantilever	Central	3000	0.16	0.1	0.001	
	Cantilever	Bottom	3000	0.16	0.1	0.001	
	Cantilever	Top	3000	0.16	0.1	0.001	
[65]	Cantilever	Central	30000	0.16	0.1	0.02	*
	Michell*	-	1000 /1000	0.5	0.5	0.02	
[75]	Cantilever	Bottom	100	0.16	0.08	-	*
[26]	Cantilever	Central	1	40	25	-	
	Cantilever	Central	1	40	25	25(v)	
	MBBB	-	1	60	20	-	
[31]	MBBB	-	100	0.05	0.05	-	
	MBBB	-	1	1	0.04	-	
[63]	Cantilever	Central	10000	3	1	0.001	
	Cantilever	-	10000	1	0.5995	0.001	

Table 2: Statistics from topology optimization literature

Article	**Test Type**	**Load region**	**Load Size**	M	L	t	**Hold Type**
[100]	Cantilever	Central	1000	10	5	-	*
	Cantilever	Central	1000	4	2	2(v)	*
[104]	Cantilever	Bottom	-	240	150	-	*
	MBBB	-	-	120	40	-	
[46]	Cantilever	Top	3000	0.16	0.1	0.001	
	Cantilever	Central	3000	0.16	0.1	0.001	
	Cantilever	Bottom	3000	0.16	0.1	0.001	
	Cantilever	-	3000	0.16	0.1	0.001	
[52]	Cantilever	Central	450	1.2	0.6	-	*
	Michell	-	1	2	1	-	
[8]	Short Cantilever	Central	-	1	1	-	
	Cantilever	Central	-	2	1	-	
[56]	Short Cantilever	Top	40	10	10	-	*
	Short Cantilever	Central	40	10	10	-	*
	Michell	-	-	100	100	-	
[21]	Two Bar	-	-	2	1	-	*
	Michell	-	-	100	100	-	
[14]	Cantilever	Top	-	2	1	-	*
	MBBB	-	-	2	1	-	*
[43]	-	-	-	-	-	-	
[47]	Michell	-	1	1	1	-	
	Cantilever	Bottom	1	2	1	-	*
[51]	-	-	-	-	-	-	
[97]	Cantilever	Central	1	2	1	1	*
	Michell	-	1	1	1.2	1	
[42]	Lshape	Central	-	-	-	-	
[86]	Cantilever	Central	1	2	1	-	*
	Michell	-	1	1	1.2	-	*
[6]	Cantilever	Central	1	2	1	-	*
	Michell	-	1	1	1.2	-	
	Michell*	-	1/1	1	1.2	-	
	Tshape	-	1	4	6	-	*
[13]	Cantilever	Top	-	2	1	-	*
	MBBB	-	-	3	1	-	*
	Michell	-	-	1.5	1	-	*
[53]	Cantilever	Central	-	2	1	-	*
[70]	Two Bar	-	1	12	4	-	*
	Lshape	Central	1	3	3	-	*
[87]	Cantilever	Central	1	2	1	-	*
	Two Bar	Central	1	2	1	-	*
[2]	Cantilever	Central	-	2	1	-	*
	Michell*	-	1/1	1	1.2	-	
[84]	Michell*	-	30/15	6	6	-	*
	Cantilever	Bottom	80	3.2	2	-	*
[82]	MBBB	-	1	3	1	1	
	Two Bar	-	1	24	10	1	*
	Cantilever	Central	1	5	3	1	*
[4]	Cantilever	Central	1	2	1	-	*
	Michell	-	1	1	1.2	-	
	Cantilever	Central	1	5	3	2.4(v)	*
	Tshape	-	-	-	-	-	*
[54]	Cantilever	Top	1000000000	4	2	1	*
	MBBB	-	1	3	1	-	
[83]	Two Bar	Central	80	2	1	-	*
	Michell*	-	30/15	6	6	-	*
[12]	Cantilever	Central	10	0.2	0.05	-	*
	MBBB	-	10	0.3	0.05	-	
[3]	Cantilever	Central	-	-	-	-	*
	Two Bar	Central	-	-	-	-(v)	*
[30]	Lshape	Central	-	-	-	-	*
	Cantilever	Top	-	-	-	-	*

Table 3: Statistics from topology optimization literature

Article	Test Type	Load region	Load Size	M	L	t	Hold Type
[73]	MBBB	-	-	3	1	-	
[102]	Cantilever	Bottom	800	34	22	-	*
	Michell*	-	300/150	6	6	-	*
	Two Bar	-	800	60	25	-	*
	Michell	-	800	60	60	-	*
	Michell	-	800	60	60	-	
	MBBB	-	80	12	4	-	*
[85]	Two Bar	-	40000	2	1	-	*
	Cantilever	Bottom	-	-	-	-	*
	MBBB	-	20000	1.2	0.4	-	*
	Michell*	-	30/5	-	-	-	*
[11]	Cantilever	Central	1	3.2	2	-	*
	MBBB	-	1	3	1	-	
[20]	-	-	-	-	-	-	
[59]	Cantilever	Central	500	0.48	0.08	0.08(v)	*
[69]	Cantilever	Central	-	8	5	-	*
	MBBB	-	-	3	1	-	*
[19]	Cantilever	Central	-	1.5	1	1(v)	*
	Cantilever	Bottom	-	1.5	1	0.4(v)	*
[10]	Cantilever	Central	-	-	-	-	*
[66]	Cantilever	Central	-	-	-	-	*
	MBBB	-	-	-	-	-	
[71]	Cantilever	Central	10	80	50	-	
	Michell*	-	10/10	20	20	1	
	Michell	-	10	20	20	1	
	MBBB	-	10	500	200	-	
[24]	Cantilever	Central	-	-	-	-	*
[9]	Cantilever	Central	-	-	-	-	*
	Cantilever	Bottom	-	-	-	-	*

Table 4: Statistics from topology optimization literature

Test	Test type	P	Q
Cantilever(Figure 1)	Central Load	8.6e4 Nw	-
	Bottom Load	6.2e4 Nw	-
	Top Load	6.2e4 Nw	-
Short Cantilever(Figure 2)	Central Load	9.0e4 Nw	-
	Bottom Load	5.8e4 Nw	-
	Top Load	5.8e4 Nw	-
LShape(Figure 3)	Central Load	1.5e4 Nw	-
	Top Load	1.5e4	-
Michell(Figure 4)	Test1	5.6e4 Nw	-
	Test2	2.8e4	-
	Test3	3.72e4	1.86e4
MBBB(Figure 5)	-	2.7e4	-
Two Bars(Figure 6)	-	15.3e4	-

Table 5: Loads values for tests

Material Properties

For the proposed tests the material used is the ASTM A-36 steel. Possibly, the most common material used in real-world structural mechanics.

- Young modulus = 2.11e11 Pa
- Poisson ratio = 0.29
- Density = 7874 kg/m3
- Yield stress = 2.2e8 Pa

4.2 Domains, dimensions and boundary conditions

Cantilever

Figure 1 show *Cantilever* domain and boundary conditions in three different fashions. This test is reported in 67 of the 103 articles reviewed. In those 67 articles there are 91 different *Cantilever* tests. In 64 of the 91, the load is at the center at the right side as in Figure 1(a), in 19 it is at the bottom at the right side as in Figure 1(b), and in 8 it is at the top at the right side as in Figure 1(c). In 19 the dimensions are the same than those in Figure 1, and in 40 the dimensions have the same relation $(R_1 : R_2) = (1 : 2)$ In 79, the displacement-conditioned segment is the same than the proposed.

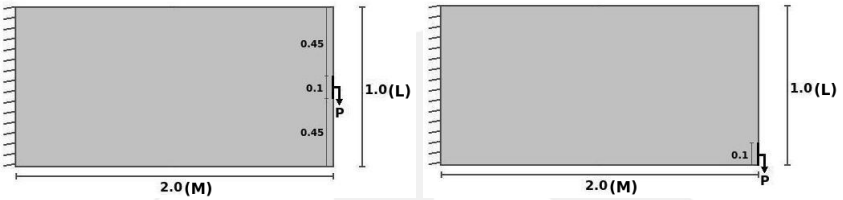

(a) Central-Load Cantilever (CLC) (b) Bottom-Load Cantilever (BLC)

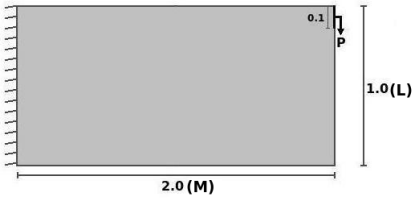

(c) Top-Load Cantilever (TLC)

Figure 1: Cantilever, (a) with a central load, (b) with a load at the bottom-right, and (c) with a load at the top-right.

Short Cantilever

Figure 2 shows the *Short Cantilever* domain and boundary conditions. This test is reported in 8 of the 103 articles reviewed. In those 8 articles there are 10 different *Short Cantilever* tests. In 2 of those 10, the load is at the center at the right side as in Figure 2(a). In 6 is at the bottom at the right as in Figure 2(b) and in 2 is at the top-right side as in Figure 2(c). In 5 the dimensions are the same than those in Figure 2, and in 10 the dimensions have the same relation $(R_1 : R_2) = (1 : 1)$. In 7, the displacement-conditioned segment is the same than the proposed.

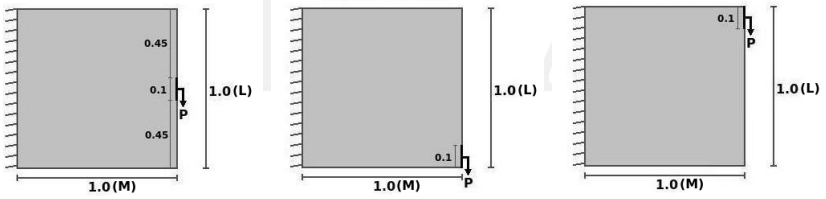

(a) Central-Load Short Cantilever (CLSC) (b) Bottom-Load Short Cantilever (BLSC) (c) Top-Load Short Cantilever (TLSC)

Figure 2: Short Cantilever, (a) with a central load, (b) with a load at the bottom-right , and (c) with a load at the top-right side.

L Shape test

Figure 3 shows the *L Shape* domain and boundary conditions. This test is reported in 20 of the 103 articles reviewed. In those 20 articles there are 21 different *L Shape* tests. In 12 cases the load is at the center

of the right-bottom side as in Figure 3(a) and in 9 is at the top of the right side as in Figure 3(b). In 8, the dimensions are the same than those in Figure 3, and in 13 the dimensions have the same relation $(R_1 : R_2) = (0.6 : 0.4)$. In 17, the displacement-conditioned segment is the same than the proposed.

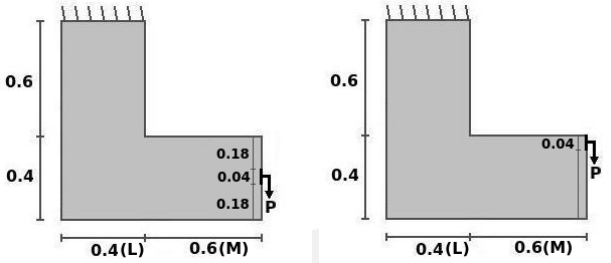

(a) Central-Load LShape (CLL) (b) Top-Load LShape (TLL)

Figure 3: L Shape, (a) with a central load, (b) with a load at the top-right.

Michell

Figure 4 shows the *Michell* domain and boundary conditions. This test is reported in 28 of the 103 articles reviewed. In 28 articles there are 32 different *Michell* tests. In 20 of those 32 there is only one load at the left-bottom side as in figure 4(a). In 7 there are two equal loads as in figure 4(b), and in 5 there are two different loads as in figure 4(c). In 7 the dimensions are the same than those in Figure 4, and in 18 the dimensions have the same relation $(R_1 : R_2) = (1 : 1)$. In 20, the displacement-conditioned segment is the same than the proposed.

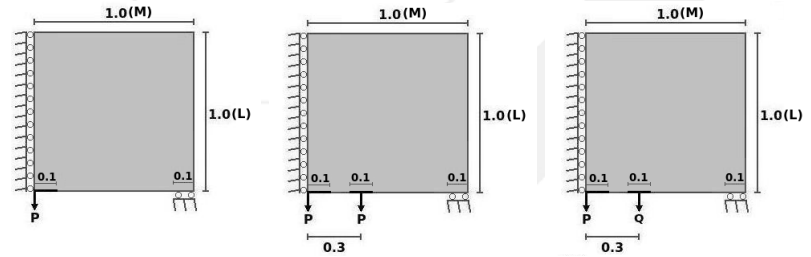

(a) One-Load Michell (OLM) (b) Two-Equal-Loads Michell (TELM) (c) Two-Different-Loads Michell (TDLM)

Figure 4: Michell, (a) with a single load, (b) with two equal loads, and (c) with two different loads.

MBBB

Figure 5 shows the *MBBB* domain and boundary conditions. This test is reported in 28 of the 103 articles reviewed. 29 different *MBBB* tests are performed in the 28 articles. All 29 tests have no differences about boundary conditions. In 8 the dimensions are the same than those in Figure 5, and in 16 the dimensions have the same relation $(R_1 : R_2) = (1 : 3)$. In 20 the displacement-conditioned segment is the same than the proposed.

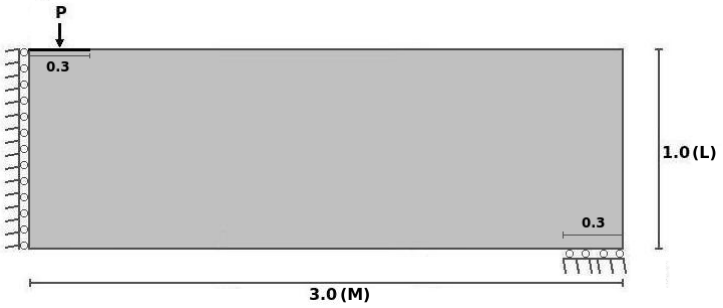

Figure 5: MBBB (MBBB)

Two Bars

Figure 6 shows the *Two Bars* domain and boundary conditions. This test is reported in 12 of the 103 articles reviewed. There are 12 different *Two Bars* tests. All 12 tests have no differences about boundary conditions. In 5 the dimensions are the same than those in Figure 6, and in 6 the dimensions have the same relation $(R_1 : R_2) = (1 : 2)$. In 12 the displacement-conditioned segment is the same than the proposed.

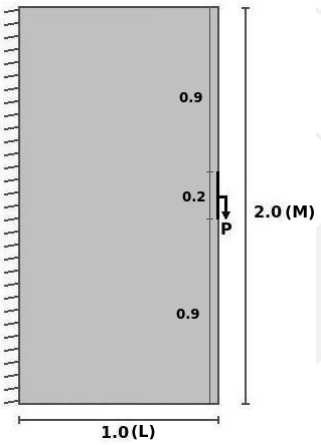

Figure 6: Two Bars (TB)

Until this section a set of problems has been well defined, the elastic behavior could be simulated with several different methods, by instance, the finite element method (FEM), the finite differences method (FDM), etc. But notice, that the numerical simulation is independent of the definition of the elastic problem. Thus, we can consider that until here the benchmark has been defined. Nevertheless, in the next subsection we propose a set of meshes for the FEM that could be used to approximate the solution.

5 Meshes

Figures 7, 8, 9, 10, 11 and 12 show meshes established for each test. On this figures, every side has the number of elements which it is divided. The meshes where defined according the following criteria:

- They must use exact square elements. As, in general, we assume that we do not known the final shape, square elements are a kind of equilibrium in numerical error cause by the element shape.
- Nodes position must allow to set exactly the boundary conditions, that is to say, we must be able to apply the load in the exact segment it is defined.
- All meshes must have at least 10000 elements in order to produce adequate numerical results and maintaining a relatively short computational solving time.

Using the shortest length side as basis, with the purpose of accomplish the conditions above, we follow the next algorithm:

1. Set a partition parameter $p = 1$.
2. The side of minimum length is partitioned in $10p$.
3. The other sides are partitioned in regard to generate square elements.
4. If the number of elements is less than 10000, increase $p = p + 1$ and go to step 2. Otherwise, the procedure stops.

Cantilever

Figure 7 shows the mesh of the Cantilever domain . The number of elements/partitions in each side is indicated. For any of the Cantilever test we propose to mesh this problem with 12800 elements of square elements with an area of 0.0125x0.0125 = 0.000156 m^2. A uniformly distributed load P is applied on 9 nodes.

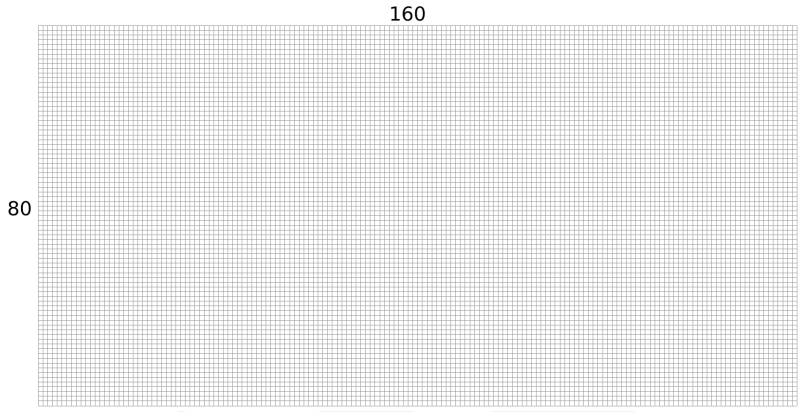

Figure 7: Cantilever mesh

Short Cantilever

Figure 8 shows the mesh of the Short Cantilever domain. The number of elements/partitions in each side is indicated. For any of the Short Cantilever test we propose to use a mesh with 10000 elements. Every square element has an area of 0.01x0.01 = 0.0001 m^2. A uniformly distributed load P is applied on 11 nodes.

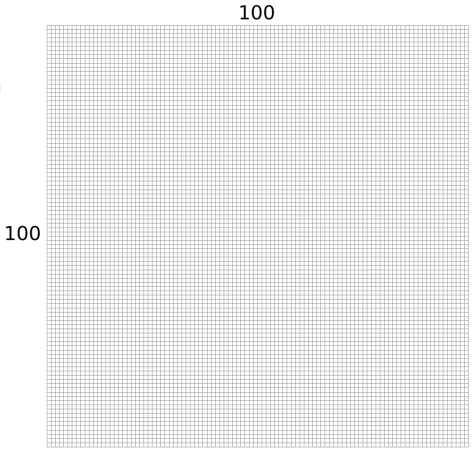

Figure 8: Short Cantilever mesh

L Shape

Figure 9 shows the mesh of the L-shape domain. The number of elements/partitions in each side is indicated. For any of the LShape test we propose a mesh with 14400 elements. Every square element has an area of 0.01x0.01 = 0.0001 m^2. A uniformly distributed load P is applied on 7 nodes in each test.

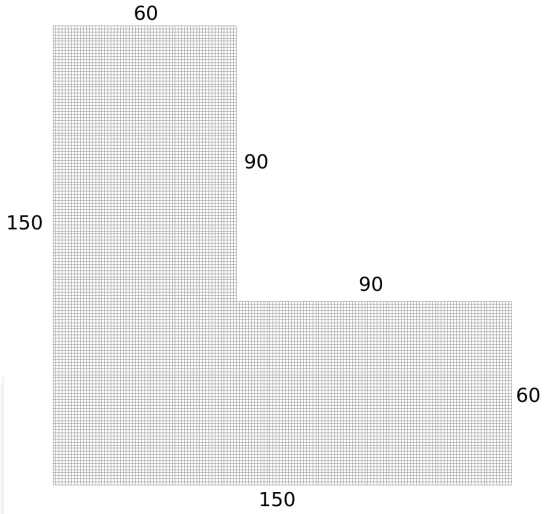

Figure 9: LShape mesh

Michell

Figure 10 shows the mesh of the Michell domain. The number of elements/partitions in each side is indicated. For any of the Michell test we propose a mesh with 14400 elements. Every square element has an area of 0.01x0.01 = 0.0001 unit^2. Uniformly distributed loads P and Q can be applied on 11 nodes in each test.

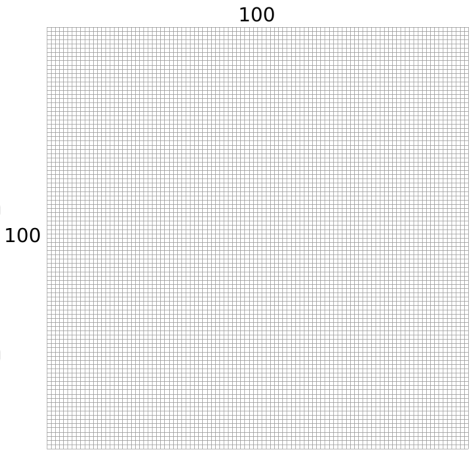

Figure 10: Michell mesh

MBBB

Figure 11 shows the mesh of the MBBB domain. The number of elements/partitions in each side is indicated. We proposed to mesh using 10800 square elements with an area of 0.01666x0.01666 = 0.0002777 m^2. A uniformly distributed load P is applied on 19 nodes.

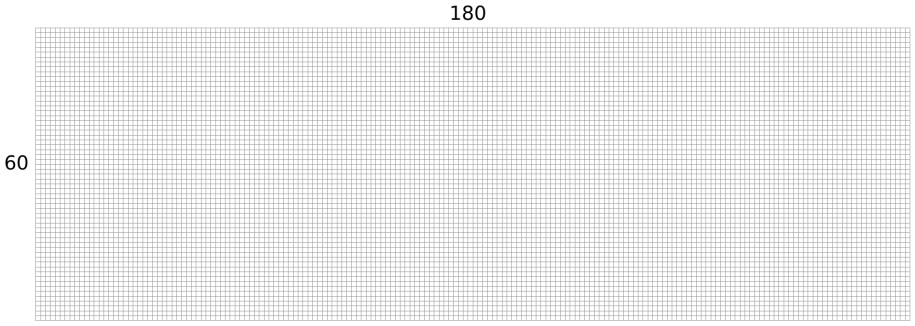

Figure 11: MBBB mesh

Two Bars

Figure 12 shows the mesh of the MBBB domain. The number of elements/partitions in each side is indicated. We propose to mesh using 12800 square elements with an area of 0.0125x0.0125 = 0.000156 m^2. A uniformly distributed load P is applied on 17 nodes.

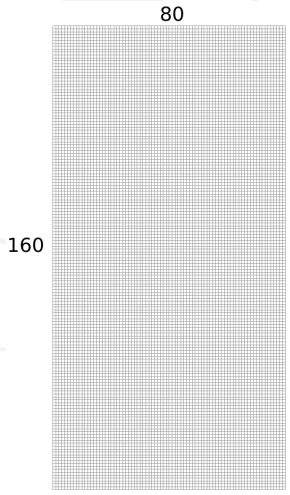

Figure 12: Two Bars mesh

6 Optimization methods and objective functions

From our point of view, there are two important objective functions in topology optimization:

- Minimization of the compliance subject to volume constraint [68].
- Minimization of volume subject to a stress constraint [7].

The first, possibly, is the most widely used optimization goal in academy, while the second, in our point of view is the most applicable approach, taking into consideration that industry most often intend to reduce cost (volume or weight) maintaining sufficient prestations. For this benchmark both goals are addressed using one of the best performed methods: the Solid Isotropic Material with Penalization (SIMP). This method is used for compliance minimization subject to a constraint of volume.

For the second goal we introduce a novel modification to the SIMP which is used to address the problem of volume minimization subject to a stress constraints. They are briefly described below.

6.1 The SIMP

The SIMP [68] is a topology optimization method based on the homogenization concept. The idea is that each finite element has a particular microstructure with its proper density and Young modulus. These properties are *homogenized* in each element through a single design variable x_i for the i element. The elemental Young modulus is usually defined as $E_i = E_0 x_i^p$ for $p \geq 3$, and density is defined as $\rho_i = \rho_0 x_i$. Where E_0 and ρ_0 are Young modulus and density, respectively, of a solid element. p is a positive integer, which is used to diminish stiffness (Young modulus) in a greater amount than density. The objective function is derived in order to establish the first optimality condition (gradient is zero in the optimum), the optimum configuration of design variables is approached y means of a fixed point iteration on the equation of the first optimality condition. Some heuristics are applied int the x_i updating in benefit of stabilizing the method.

We have implemented two different SIMP algorithm, the first one is the same than in [68], the second one has a difference in the stopping criterion. Since SIMP is a fixed point-heuristic method, hence a usual criterion for this kind of methods (and the used one in [68]) is when $x = f(x)$, in the case of the SIMP where $f(x)$ is the update of design variables), so convergence criterion used for SIMP is $||x - f(x)|| < e_0$, this means that design variables negligible change in two consecutive iterations. Although, the parameter e_0 must be tuned for each particular problem, and there are not a simple rule to set the value in an inexpensive and straight forward manner. If one sets an e_0 parameter sufficiently small to guaranty adequate convergence in all the cases, it is quite possible that, in many cases, the structure has almost reached its final configuration, the compliance $F(x)$ is quite similar between consecutive iterations, but the established convergence criteria is not reached.

In order to circumvent this issue we use another stopping criteria, the algorithm stops if both of the following are reached: a) The absolute difference of Security Factor(FS mentioned in section 4.1) between two consecutive iterations: $|SF^{k-1} - SF^k| < e$ where k is the iteration number, and b) The variance given by: $\frac{1}{v}\sum_{i=1}^{v}(G(x)_i - \hat{G(x)})^2 < e$ where $G(x)$ is the group of the compliance calculated in the last v iterations, this means that compliance in the last v iterations are similar. We have named this version SIMP with Stress and Variance Convergence: SIMPSVC.

6.2 SIMP for volume minimization subject to a stress constraint (SIMPSC)

In contemplation of applying the SIMPSVC for minimum volume subject to a stress constraint. We follow the next algorithm:

1. Set the volume fraction in the SIMPSVC to 0.5.
2. Execute the SIMP SVC using the convergence criteria as described above.
3. If the security factor SF of the final structure is less than 1 the volume fraction is decreased, if SF is greater than 1 the volume fraction is increased. The volume fraction, V^k, is increased or decreased a fraction ΔV^k by means of a classic bisection method in the interval $[0, 1]$, with initial point at 0.5.
4. The SIMPSC stops if a) The final security factor of the SIMP SVC $0 < 1.0 - SF^k < e$ and $SF^k < 1$, or b) $\Delta V^k < e$ and $SF^k < 1$ or c) If $k > iter_{max}$, where $iter_{max}$ is the maximum number of iterations. Otherwise, repeat from step 2.

7 Benchmark results

In this section we present results for the SIMP, SIMPSVC and the SIMPSC. They are reported from Table 6 to 18. The parameters for the SIMP (using the nomenclature in [68]), SIMPSVC and SIMPSC are: a) $p = 3$, b) $m = 0.2$, c) $r_{min} = 0.05$ (used for neighborhoods in filtering) d) ΔV^k is reported in tables as *Final Volume Fraction*, e) $v = 5$,f) $e = 1.0e-2$ for SIMP and $e = 1.0e-3$ for SIMPSVC and SIMPSC, and g) $iter_{max} = 150$ for SIMP and SIMP SVC and $iter_{max} = 250$ for SIMPSC. All tests were done using an *Intel Core i7-2600 CPU @ 3.40GHz x 8* with *3.8 GiB RAM memory* using *Ubuntu 14.04 LTS, 64 bits OS*.

In result tables we report the following information: row 1) Initial Security Factor, this is calculated with the whole domain with all design variables equal to 1. It is the same for SIMPSC and SIMP and relevant only for SIMPSC. row 2) Number of iterations. row 3) Initial volume. row 4) Final Volume. row 5) Final volume fraction, which is also the volume constraint for SIMP. row 6) Final compliance reached. row 7) Average of

the of X displacements in nodes with external forces. row 8) Average of absolute X displacement in nodes with external forces. row 9) Average of Y displacements in nodes with external forces. row 10) Average of absolute Y displacements in nodes with external forces. row 11) Average of norms of displacements in nodes with external forces. row 12) Security factor in the last iteration. row 13) and row 14) Average and standard deviation of elemental von Mises stress over yield stress. This value gives a general idea of efficiency of the structure, the most efficient structure has an average of 1 and standard deviation of 0. row 14) Maximum elemental Von Mises stress in structure. The last four values are not relevant for the SIMP and SIMP SVC, because stress is not considered in this method. In addition we report five figures for each test problem: histograms of the von Mises stress over yield stress for the SIMP,SIMPSVC and SIMPSC.

7.1 Cantilever with load at center (CLC)

Data	SIMPSC	SIMPSVC	SIMP
Initial SF	7.494793 e-1	-	-
Iterations	176	42	150
Initial Volume	2.0e0	2.0e0	2.0e0
Final Volume	1.271483e0	1.0e0	1.0e0
Final Volume fraction	6.357417e-1	5.0e-1	5.0e-1
Compliance	1.847301e2	2.3086e2	2.3029e2
X displacement avg	-3.2311e-10	-1.9895e-10	-6.7693e-10
X displacement abs avg	3.7892e-5	4.3923e-5	4.5094e-5
Y displacement avg	-1.9256e-2	-2.4083e-2	-2.4024e-2
Y displacement abs avg	1.9256e-2	2.4083e-2	2.4024e-2
|Displacement|	2.14007e-3	2.6764e-3	2.6698e-3
Security Factor	9.996258e-1	1.2499e0	1.2435e0
Avg(VM/YS)	2.2621e-1	3.4061e-1	3.3977e-1
SD(VM/YS)	6.9561e-2	7.2220e-2	7.2117e-2
Max VonMises	2.199177e8	2.7499e8	2.7357e8

Table 6: CLC execution data

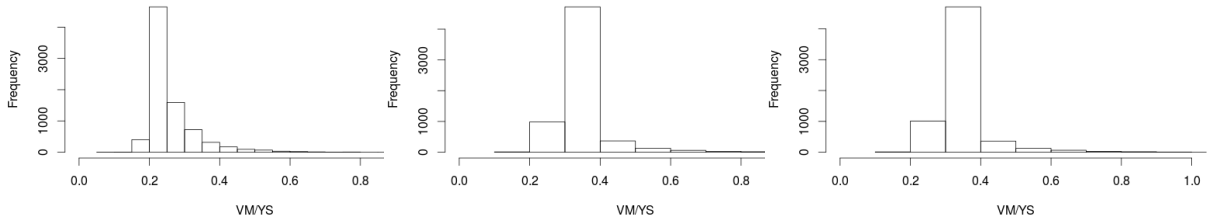

(a) SIMPSC (b) *SIMPSVC, exceeds yield stress (c) *SIMP, exceeds yield stress

Figure 13: CLC: VM/YS elemental histogram

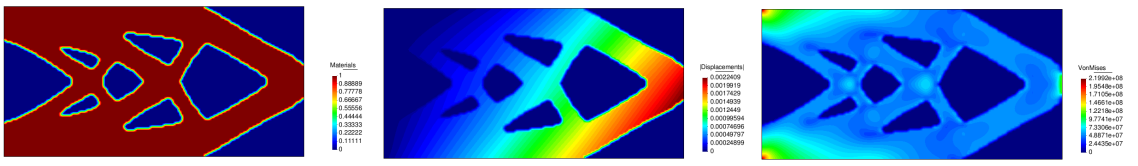

(a) CLC material (b) CLC displacements (c) CLC VonMises

Figure 14: CLC visual results with SIMPSC

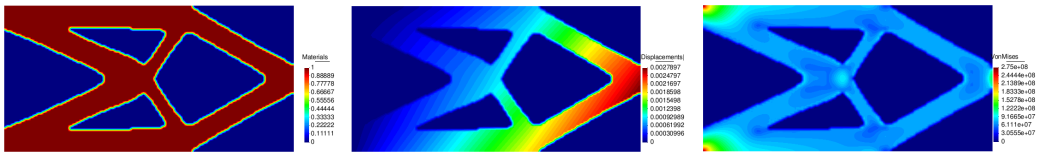

(a) CLC material (b) CLC displacements (c) CLC VonMises

Figure 15: CLC visual results with SIMPSVC

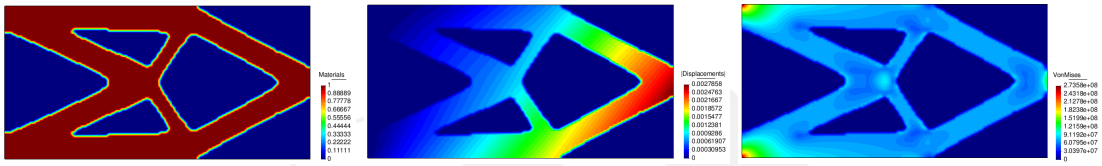

(a) CLC material (b) CLC displacements (c) CLC VonMises

Figure 16: CLC visual results with SIMP

7.2 Cantilever with load at bottom (CLB)

Data	SIMPSC	SIMPSVC	SIMP
Initial SF	7.526465e-1	-	
Iterations	167	39	150
Initial Volume	2.0e0	2.0e0	2.0e0
Final Volume	9.25782e-1	1.0e0	1.0e0
Final Volume fraction	4.6289e-1	5.0e-1	5.0e-1
Compliance	1.3955e+2	1.2911e2	1.2828e2
X displacement avg	-5.6312e-4	-5.3832e-4	-5.3654e-4
X displacement abs avg	5.6312e-4	5.3832e-4	5.3654e-4
Y displacement avg	-2.0173e-2	-1.8660e-2	-1.8540e-2
Y displacement abs avg	2.0173e-2	1.8660e-2	1.8540e-2
|Displacement|	2.311752e-3	2.1427e-3	2.1293e-3
Security Factor	9.968923e-1	9.21841e-1	9.1895e-1
Avg(VM/YS)	2.7648e-1	2.5631e-1	2.5515e-1
SD(VM/YS)	5.6441e-2	5.4746e-2	5.4179e-2
Max VonMises	2.193163e8	2.02805e8	2.0216e8

Table 7: CLB execution data

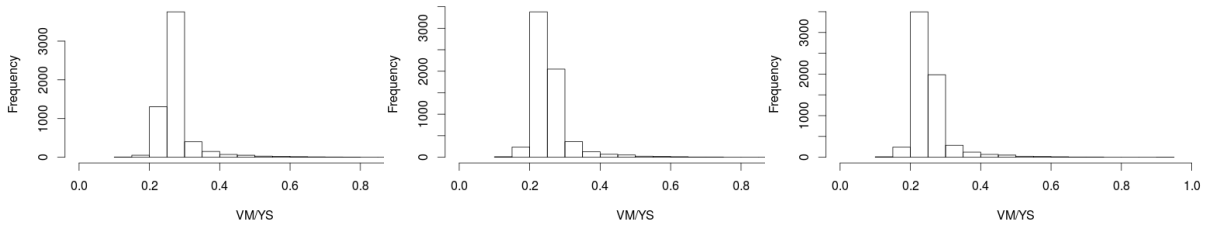

(a) SIMPSC (b) SIMPSVC (c) SIMP

Figure 17: CLB: VM/YS elemental histogram

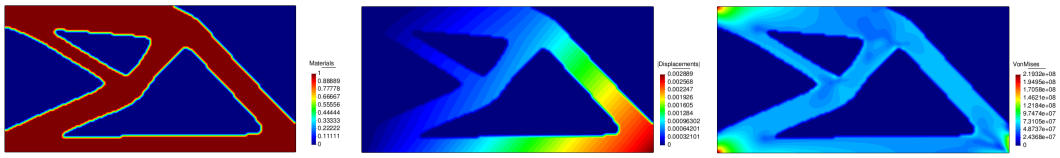

(a) CLB material (b) CLB displacements (c) CLB VonMises

Figure 18: CLB visual results with SIMPSC

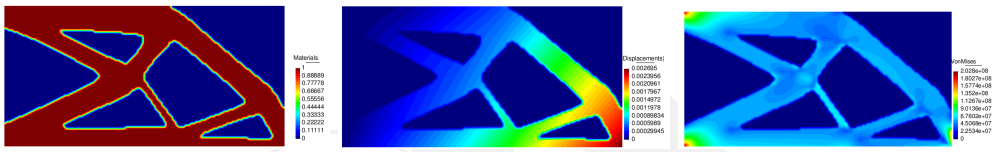

(a) CLB material (b) CLB displacements (c) CLB VonMises

Figure 19: CLB visual results with SIMPSVC

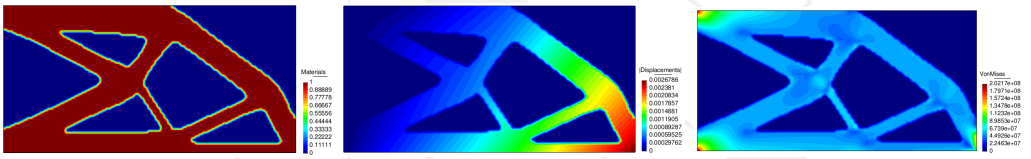

(a) CLB material (b) CLB displacements (c) CLB VonMises

Figure 20: CLB visual results with SIMP

7.3 Cantilever with load at top (CLT)

Data	SIMPSC	SIMPSVC	SIMP
Initial SF	7.526465e-1	-	-
Iterations	167	39	150
Initial Volume	2.0e0	2.0e0	2.0e0
Final Volume	9.257e-1	1.0e0	1.0e0
Final Volume fraction	4.6289e-1	5.0e-1	5.0e-1
Compliance	1.395586e2	1.29112e2	1.2828e2
X displacement avg	5.6312e-4	5.3832e-4	5.3656e-4
X displacement abs avg	5.6312e-4	5.3832e-4	5.3656e-4
Y displacement avg	-2.0173e-2	-1.8659e-2	-1.8540e-2
Y displacement abs avg	2.0173e-2	1.8659e-2	1.8540e-2
|Displacement|	2.3117e-3	2.1426e-3	2.1293e-3
Security Factor	9.968896e-1	9.2182e-1	91892e-1
Avg(VM/YS)	2.7649e-1	2.5630e-1	2.5513e-1
SD(VM/YS)	5.6441e-2	5.4744e-2	5.4175e-2
Max VonMises	2.193157e8	2.0280e8	2.0216e8

Table 8: CLT execution data

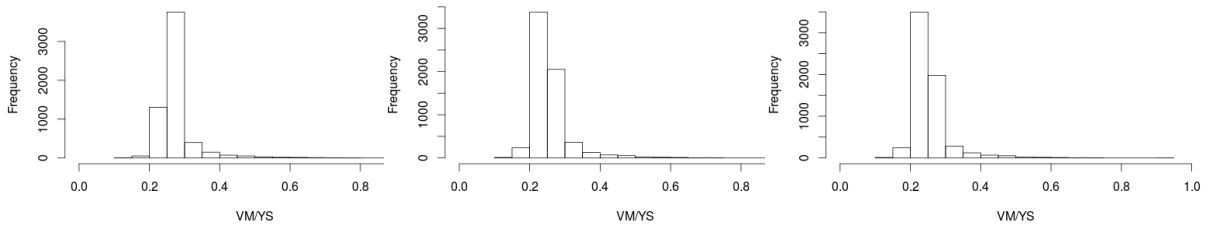

(a) SIMPSC (b) SIMPSVC (c) SIMP

Figure 21:

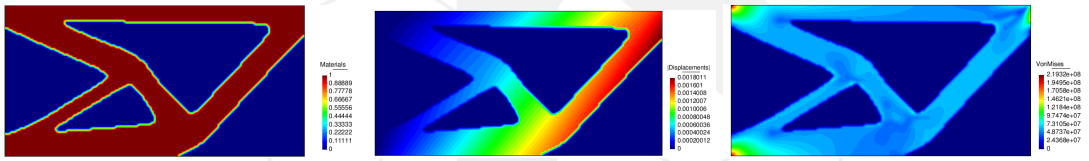

(a) CLT material (b) CLT displacements (c) CLT VonMises

Figure 22: CLT visual results with SIMPSC

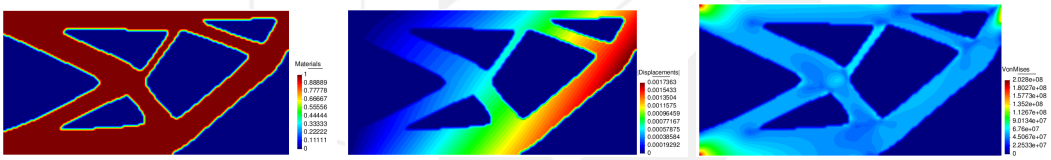

(a) CLT material (b) CLT displacements (c) CLT VonMises

Figure 23: CLT visual results with SIMPSVC

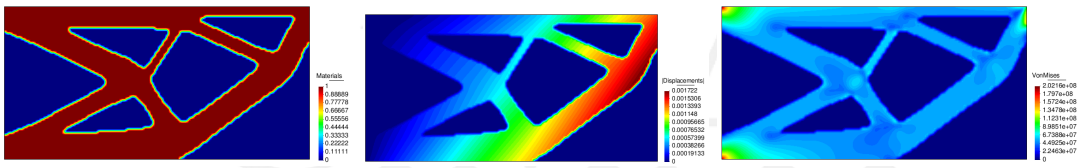

(a) CLT material (b) CLT displacements (c) CLT VonMises

Figure 24: CLT visual results with SIMP

7.4 Short Cantilever with load at center(SCLC)

Data	SIMPSC	SIMPSVC	SIMP
Initial SF	7.5516e-1	-	-
Iterations	138	27	150
Initial Volume	1.0e0	1.0e0	1.0e0
Final Volume	4.3945e-1	5.0e-1	5.0e-1
Final Volume fraction	4.39453e-1	5.0e-1	5.0e-1
Compliance	6.29219e1	5.6125e1	5.6164e1
X displacement avg	9.6287e-9	-1.2925e-8	6.2024e-9
X displacement abs avg	1.8152e-5	1.5652e-5	1.5125e-5
Y displacement avg	-7.6768e-3	-6.8468e-3	-6.8517e-3
Y displacement abs avg	7.6768e-3	6.8468e-3	6.8517e-3
|Displacement|	6.9821e-4	6.2271e-4	6.2313e-4
Security Factor	9.9822e-1	9.0120e-1	8.9053e-1
Avg(VM/YS)	2.7610e-1	2.4709e-1	2.4739e-1
SD(VM/YS)	5.4350e-2	5.2463e-2	5.0792e-2
Max VonMises	2.196099e8	1.9826e8	1.9591e8

Table 9: SCLC execution data

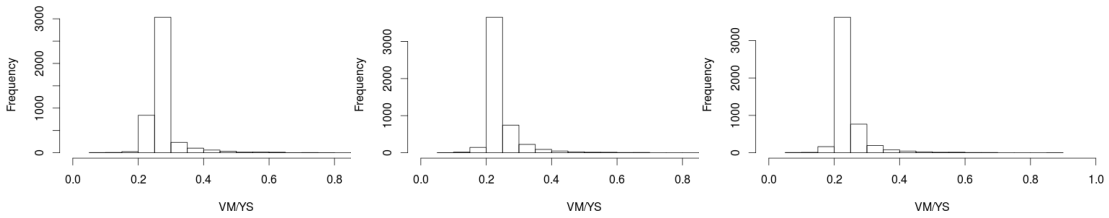

(a) SIMPSC (b) SIMPSVC (c) SIMP

Figure 25: SCLC: VM/YS elemental histogram

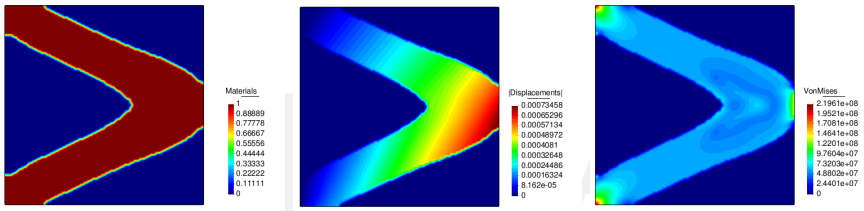

(a) SCLC material (b) SCLC displacements (c) SCLC VonMises

Figure 26: SCLC visual results with SIMPSC

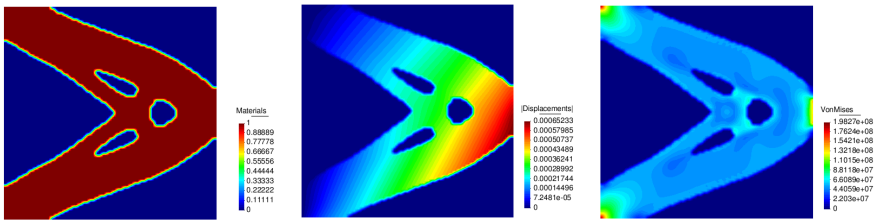

(a) SCLC material (b) SCLC displacements (c) SCLC VonMises

Figure 27: SCLC visual results with SIMPSVC

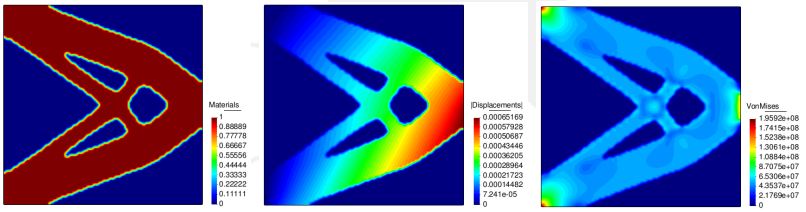

(a) SCLC material (b) SCLC displacements (c) SCLC VonMises

Figure 28: SCLC visual results with SIMP

7.5 Short Cantilever with load at bottom(SCLB)

Data	SIMPSC	SIMPSVC	SIMP
Initial SF	7.4841e-1	-	-
Iterations	139	23	150
Initial Volume	1.0e0	1.0e0	1.0e0
Final Volume	2.63672e-1	5.0e-1	5.0e-1
Final Volume fraction	2.63672e-1	5.0e-1	5.0e-1
Compliance	5.7462e1	2.828671e1	2.8305e1
X displacement avg	-3.2983e-4	-1.6440e-4	-1.6480e-4
X displacement abs avg	3.2983e-4	1.6440e-4	1.6480e-4
Y displacement avg	-1.0880e-2	-5.3506e-3	-5.3544e-3
Y displacement abs avg	1.0880e-2	5.3506e-3	5.3544e-3
|Displacement|	1.0429e-3	5.1400e-4	5.1445e-4
Security Factor	9.9849e-1	7.2492e-1	7.2553e-1
Avg(VM/YS)	3.7022e-1	1.6864e-1	1.6906e-1
SD(VM/YS)	4.4009e-2	4.3037e-2	4.2259e-2
Max VonMises	2.196685e8	1.5948e8	1.5931e8

Table 10: SCLB execution data

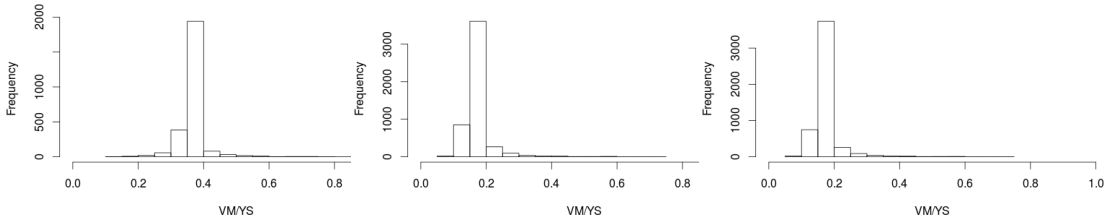

(a) SIMPSC (b) SIMPSVC (c) SIMP

Figure 29: SCLB: VM/YS elemental histogram

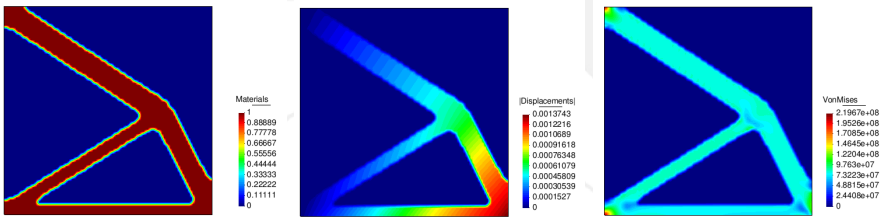

(a) SCLB material (b) SCLB displacements (c) SCLB VonMises

Figure 30: SCLB visual results with SIMPSC

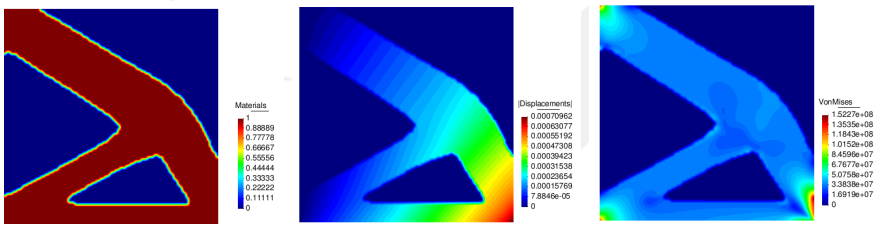

(a) SCLB material (b) SCLB displacements (c) SCLB VonMises

Figure 31: SCLB visual results with SIMPSVC

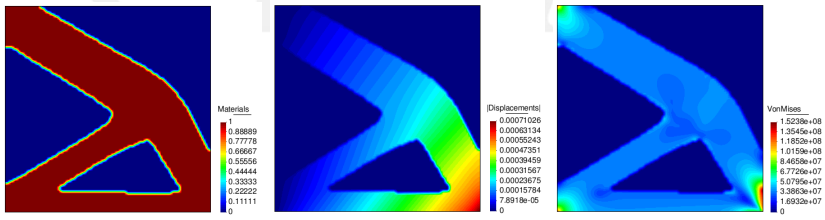

(a) SCLB material (b) SCLB displacements (c) SCLB VonMises

Figure 32: SCLB visual results with SIMP

7.6 Short Cantilever with load at top(SCLT)

Data	SIMPSC	SIMPSVC	SIMP
Initial SF	7.48413e-1	-	-
Iterations	139	23	150
Initial Volume	1.0e0	1.0e0	1.0e0
Final Volume	2.6367e-1	5.0e-1	5.0e-1
Final Volume fraction	2.6367e-1	5.0e-1	5.0e-1
Compliance	5.74511e1	2.8285e1	2.830491e1
X displacement avg	3.2972e-4	1.6439e-4	1.6482e-4
X displacement abs avg	3.2972e-4	1.6439e-4	1.6482e-4
Y displacement avg	-1.0878e-2	-5.3504e-3	-5.3543e-3
Y displacement abs avg	1.0878e-2	5.3504e-3	5.3543e-3
|Displacement|	1.0427e0-3	5.1398e-4	5.1445e-4
Security Factor	9.9795e-1	7.2490e-1	7.2551e-1
Avg(VM/YS)	3.7014e-1	1.6863e-1	1.6905e-1
SD(VM/YS)	4.3981e-2	4.3037e-2	4.2255e-2
Max VonMises	2.195505e8	1.5947e8	1.5961e8

Table 11: SCLT execution data

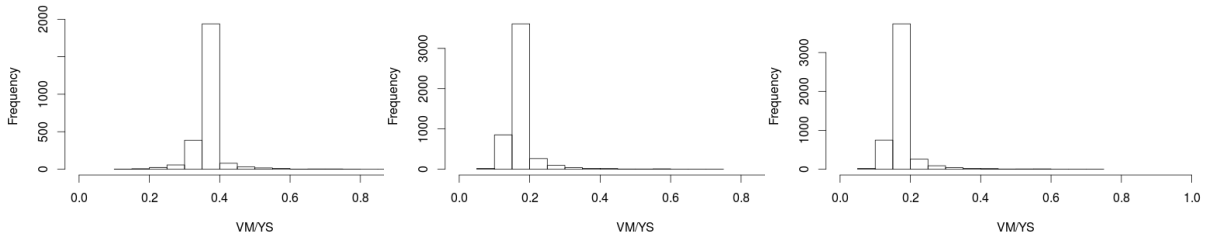

(a) SIMPSC (b) SIMPSVC (c) SIMP

Figure 33: SCLT: VM/YS elemental histogram

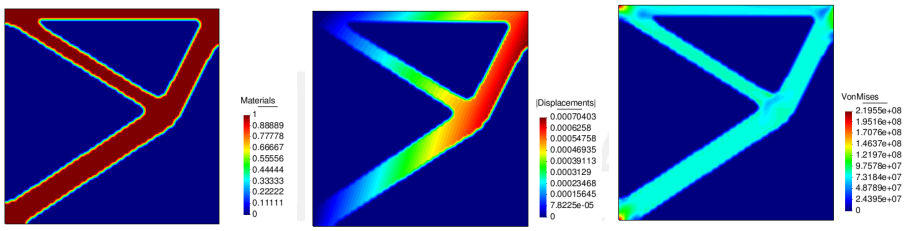

(a) SCLT material (b) SCLT displacements (c) SCLT VonMises

Figure 34: SCLT visual results with SIMPSC

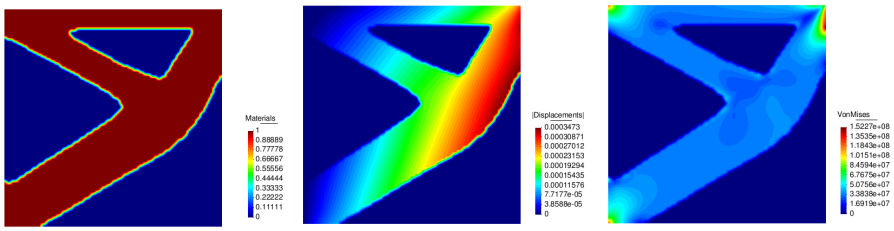

(a) SCLT material (b) SCLT displacements (c) SCLT VonMises

Figure 35: SCLT visual results with SIMPSVC

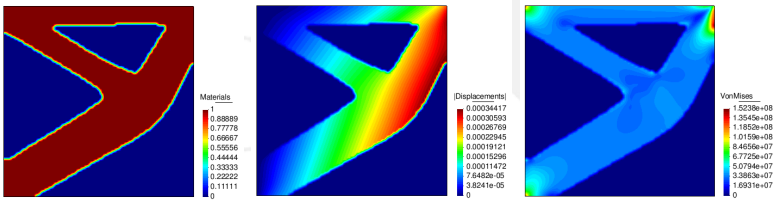

(a) SCLT material (b) SCLT displacements (c) SCLT VonMises

Figure 36: SCLT visual results with SIMP

7.7 LShape with load at center(LLC)

Data	SIMPSC	SIMPSVC	SIMP
Initial SF	7.5569e-1	-	-
Iterations	170	30	150
Initial Volume	6.4e-1	6.4e-1	6.4e-1
Final Volume	2.91253e-1	3.2e-1	3.2e-1
Final Volume fraction	4.5508e-1	5.0e-1	5.0e-1
Compliance	2.32316e1	2.0906e1	2.0794e1
X displacement avg	-5.8670e-4	-5.1391e-4	-5.1657e-4
X displacement abs avg	5.8670e-4	5.1391e-4	5.1657e-4
Y displacement avg	-1.0810e-2	-9.7257e-3	-9.6748e-3
Y displacement abs avg	1.0810e-2	9.7257e-3	9.6748e-3
|Displacement|	1.6459e-3	1.4816e-3	1.4757e-3
Security Factor	9.980207e-1	9.4391e-1	9.3930e-1
Avg(VM/YS)	2.1641e-1	1.8954e-1	1.8868e-1
SD(VM/YS)	4.2650e-2	3.9668e-2	3.9945e-2
Max VonMises	2.19564e8	2.0766e8	2.0664e8

Table 12: LLC execution data

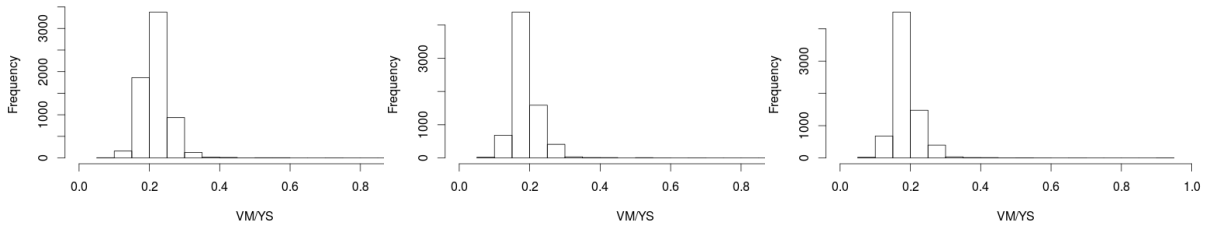

(a) SIMPSC (b) SIMPSVC (c) SIMP

Figure 37: LLC: VM/YS elemental histogram

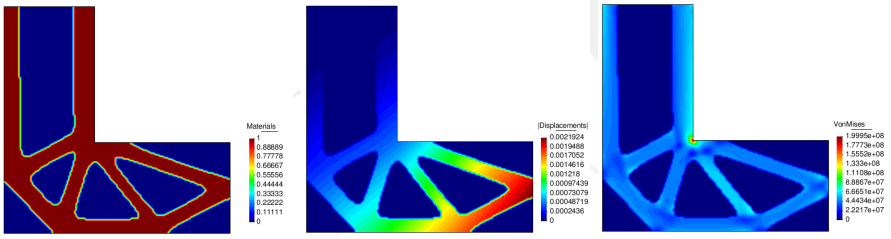

(a) LLC material (b) LLC displacements (c) LLC VonMises

Figure 38: LLC visual results with SIMPSC

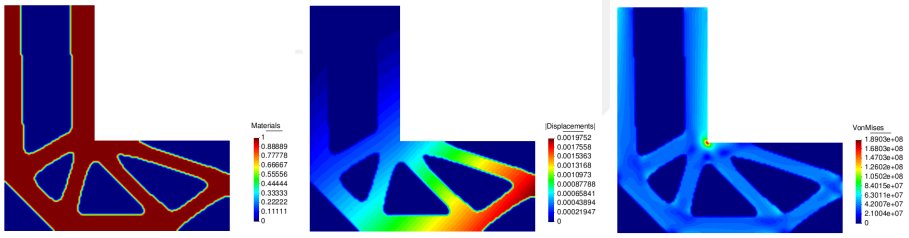

(a) LLC material (b) LLC displacements (c) LLC VonMises

Figure 39: LLC visual results with SIMPSVC

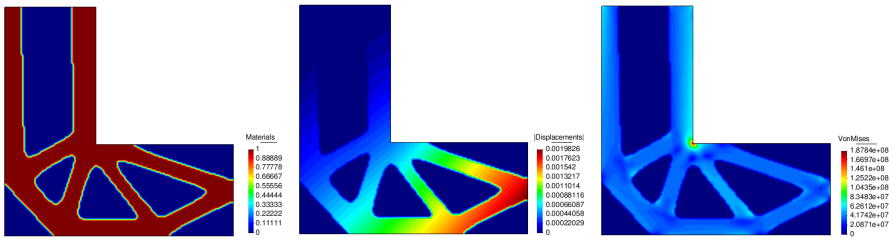

(a) LLC material (b) LLC displacements (c) LLC VonMises

Figure 40: LLC visual results with SIMP

7.8 LShape with load at top(LLT)

Data	SIMPSC	SIMPSVC	SIMP
Initial SF	7.55501e-1	-	-
Iterations	183	28	150
Initial Volume	6.4e-1	6.4e-1	6.4e-1
Final Volume	2.7246e-1	3.2e-1	3.2e-1
Final Volume fraction	4.25724e-1	5.0e-1	5.0e-1
Compliance	2.53894e1	2.01911e1	2.1044e1
X displacement avg	-1.8755e-4	-1.6784e-4	-1.6760e-4
X displacement abs avg	1.8755e-4	1.6784e-4	1.6760e-4
Y displacement avg	-1.1819e-2	-9.8113e-3	-9.7886e-3
Y displacement abs avg	1.1819e-2	9.8113e-3	9.7886e-3
|Displacement|	1.6992e-3	1.4119e-3	1.4087e-3
Security Factor	9.9995e-1	9.0702e-1	9.0651e-1
Avg(VM/YS)	2.3528e-1	1.8814e-1	1.8762e-1
SD(VM/YS)	4.1240e-2	3.8693e-2	3.8581e-2
Max VonMises	-2.19989e8	1.9954e8	1.9943e8

Table 13: LLT execution data

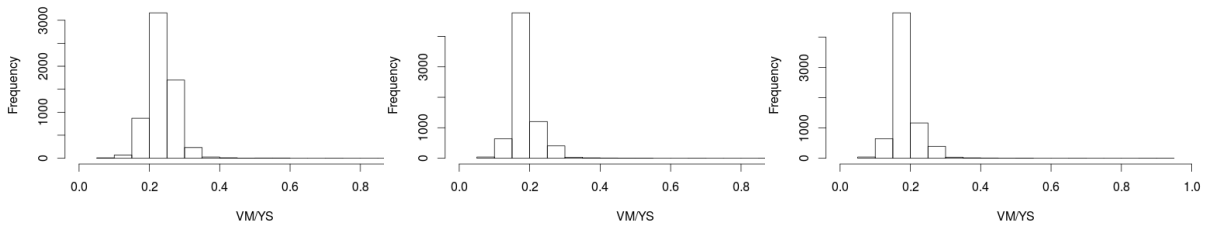

(a) SIMPSC (b) SIMPSVC (c) SIMP

Figure 41: LLT: VM/YS elemental histogram

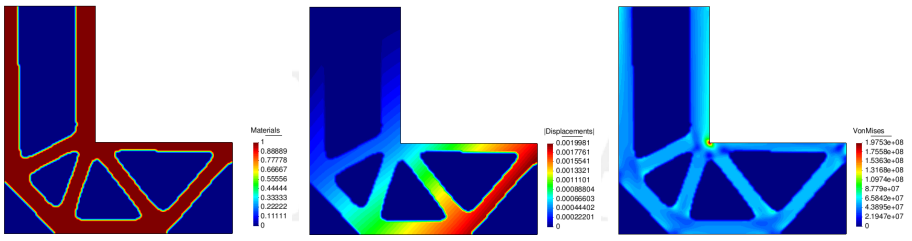

(a) LLT material (b) LLT displacements (c) LLT VonMises

Figure 42: LLT visual results with SIMPSC

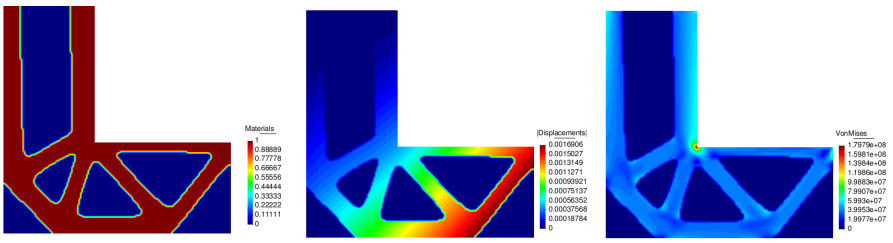

(a) LLT material (b) LLT displacements (c) LLT VonMises

Figure 43: LLT visual results with SIMSVCP

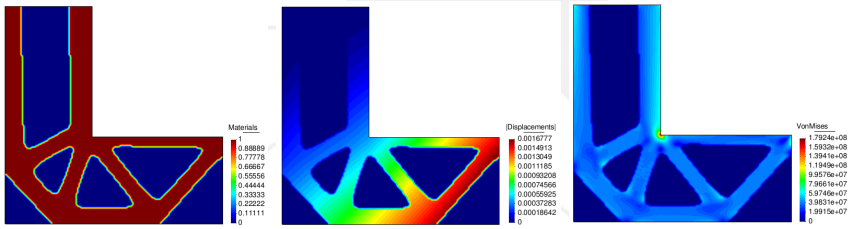

(a) LLT material (b) LLT displacements (c) LLT VonMises

Figure 44: LLT visual results with SIMP

7.9 One-Load Michell

Data	SIMPSC	SIMPSVC	SIMP
Initial SF	7.5248e-1	-	-
Iterations	138	30	150
Initial Volume	1.0e0	1.0e0	1.0e0
Final Volume	4.4531e-1	5.0e-1	5.0e-1
Final Volume fraction	4.4531e-1	5.0e-1	5.0e-1
Compliance	3.2247e+1	2.8184e1	2.7777e1
X displacement avg	1.9085e-5	1.7803e-5	1.7974e-5
X displacement abs avg	1.9085e-5	1.7803e-5	1.7974e-5
Y displacement avg	-6.3126e-3	-5.5149e-3	-5.4353e-3
Y displacement abs avg	6.3126e-3	5.5149e-3	5.4353e-3
|Displacement|	5.7431e-4	5.0180e-4	4.9457e-4
Security Factor	9.9963e-1	9.3160e-1	9.2516e-1
Avg(VM/YS)	2.0239e-1	1.7432e-1	1.7361e-1
SD(VM/YS)	3.7517e-2	3.6663e-2	3.6530e-2
Max VonMises	2.1992e8	2.0495e8	2.0353e8

Table 14: OLM execution data

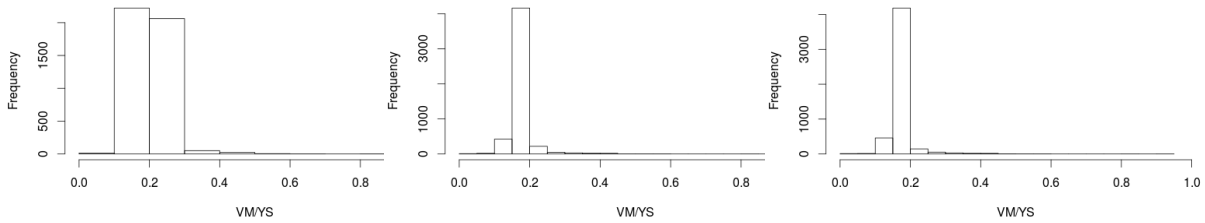

(a) SIMPSC (b) SIMPSVC (c) SIMP

Figure 45: OLM: VM/YS elemental histogram

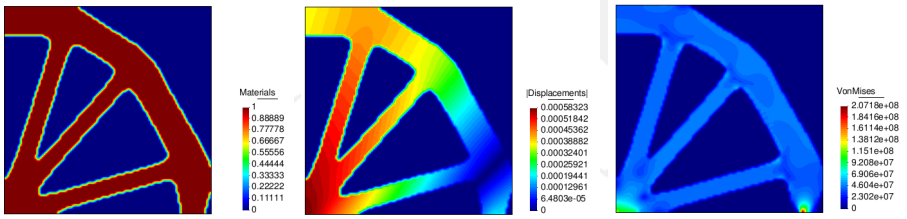

(a) OLM material (b) OLM displacements (c) OLM VonMises

Figure 46: OLM visual results with SIMPSC

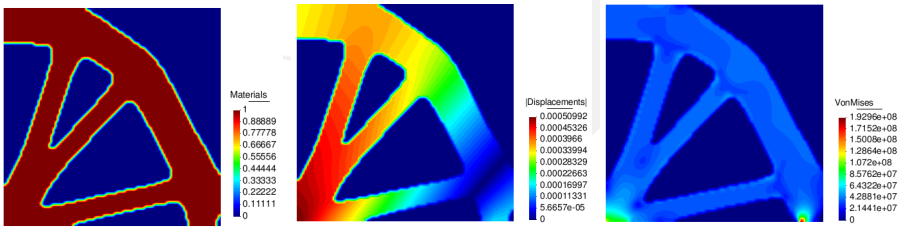

(a) OLM material (b) OLM displacements (c) OLM VonMises

Figure 47: OLM visual results with SIMPSVC

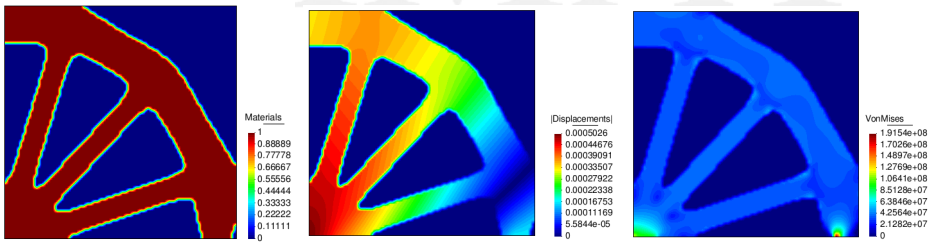

(a) OLM material (b) OLM displacements (c) OLM VonMises

Figure 48: OLM visual results with SIMP

7.10 Two-Equal-Loads Michell

Data	SIMPSC	SIMPSVC	SIMP
Initial SF	7.4867e-1	-	-
Iterations	156	29	150
Initial Volume	1.0e0	1.0e0	1.0e0
Final Volume	4.082e-1	5.0e-1	5.0e-1
Final Volume fraction	4.082e-1	5.0e-1	5.0e-1
Compliance	2.9077e1	2.2515e1	2.2538e1
X displacement avg	4.6020e-5	3.8176e-5	3.8311e-5
X displacement abs avg	4.6020e-5	3.8176e-5	3.8311e-5
Y displacement avg	-1.1384e-2	-8.8085e-3	-8.8171e-3
Y displacement abs avg	1.1384e-2	8.8085e-3	8.8171e-3
|Displacement|	5.2082e-4	4.0333e-4	4.0367e-4
Security Factor	9.9362e-1	9.0963e-1	9.0184e-1
Avg(VM/YS)	2.0362e-1	1.5617e-1	1.5654e-1
SD(VM/YS)	3.2775e-2	2.9895e-2	2.9579e-2
Max VonMises	2.18159e+8	2.0012e8	1.9840e8

Table 15: TELM execution data

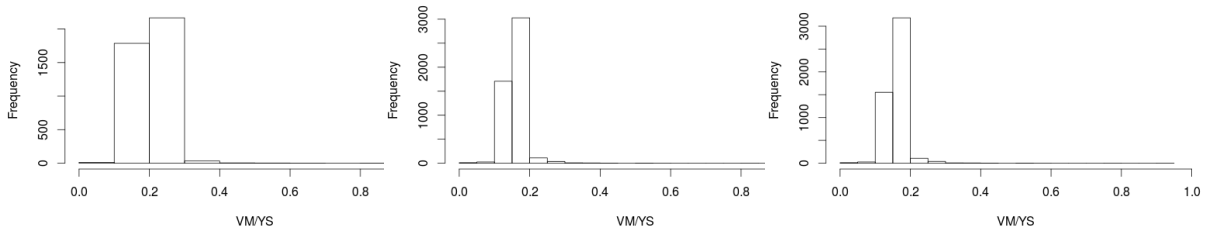

(a) SIMPSC (b) SIMPSVC (c) SIMP

Figure 49: TELM: VM/YS elemental histogram

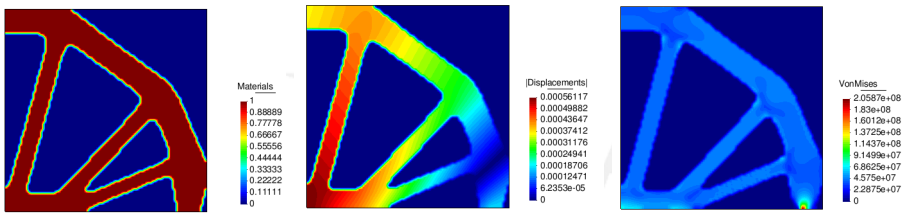

(a) TELM material (b) TELM displacements (c) TELM VonMises

Figure 50: TELM visual results with SIMPSC

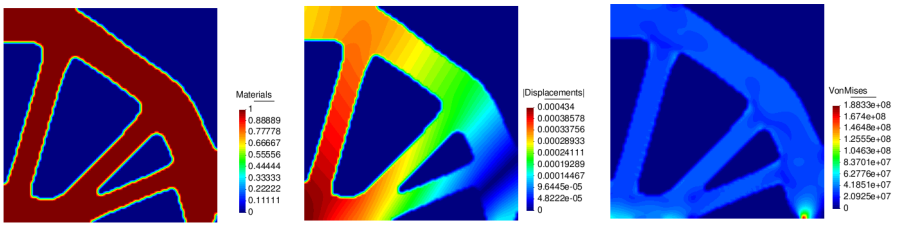

(a) TELM material (b) TELM displacements (c) TELM VonMises

Figure 51: TELM visual results with SIMPSVC

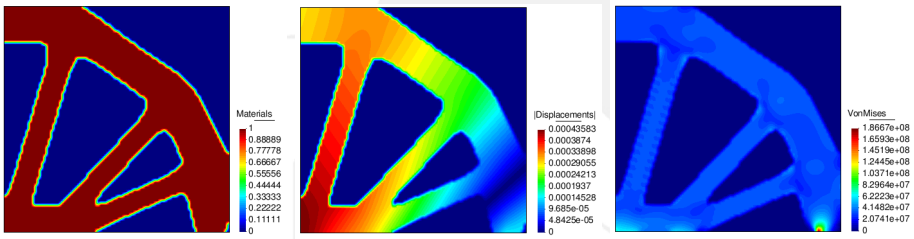

(a) TELM material (b) TELM displacements (c) TELM VonMises

Figure 52: TELM visual results with SIMP

7.11 Two-Different-Loads Michell

Data	SIMPSC	SIMPSVC	SIMP
Initial SF	7.4729e-1	-	-
Iterations	130	29	150
Initial Volume	1.0e0	1.0e0	1.0e0
Final Volume	4.1601e-1	5.0e-1	5.0e-1
Final Volume fraction	4.1601e-1	5.0e-1	5.0e-1
Compliance	2.9675e1	2.3782e1	2.3804e1
X displacement avg	4.6116e-5	3.9801e-5	3.9140e-4
X displacement abs avg	4.6116e-5	3.9801e-5	3.9140e-4
Y displacement avg	-1.1274e-2	-9.0578e-3	-9.0486e-3
Y displacement abs avg	1.1274e-2	9.0578e-3	9.0486e-3
|Displacement|	5.1584e-4	4.1483e-4	4.1426e-4
Security Factor	9.9502e-1	9.2524e-1	9.1705e-1
Avg(VM/YS)	1.9987e-1	1.5972e-1	1.6052e-1
SD(VM/YS)	3.4099e-2	3.3142e-2	3.0831e-2
Max VonMises	2.1890e8	2.0355e8	2.0175e8

Table 16: TDLM execution data

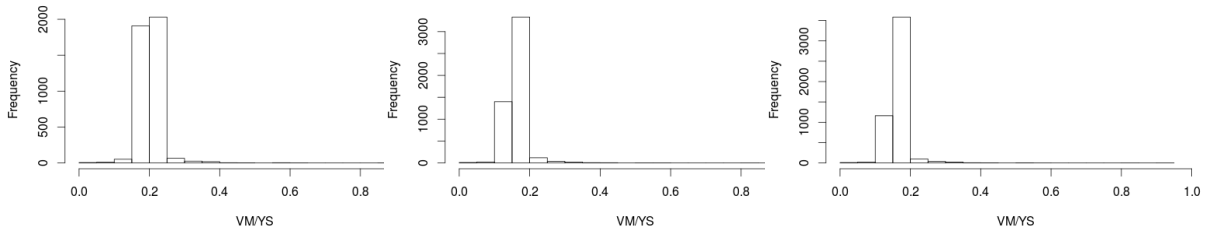

(a) SIMPSC (b) SIMPSVC (c) SIMP

Figure 53: TDLM VM/YS elemental histogram

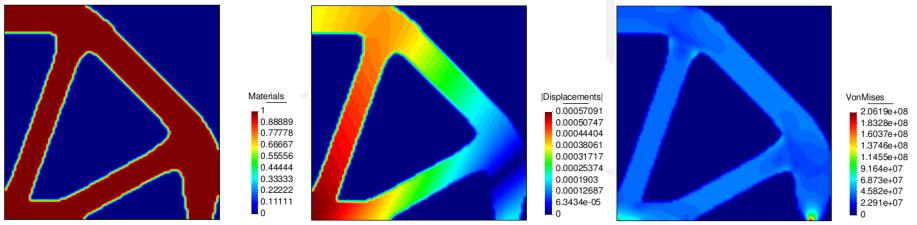

(a) TDLM material (b) TDLM displacements (c) TDLM VonMises

Figure 54: TDLM visual results with SIMPSC

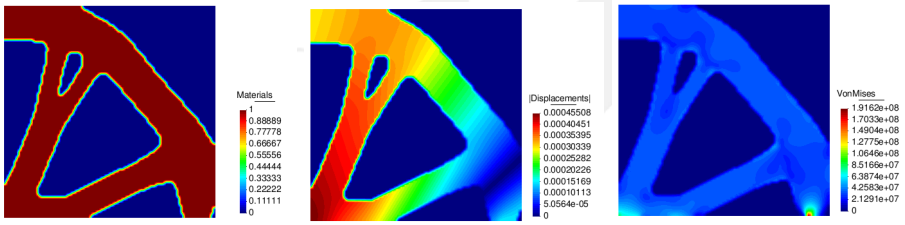

(a) TDLM material (b) TDLM displacements (c) TDLM VonMises

Figure 55: TDLM visual results with SIMPSVC

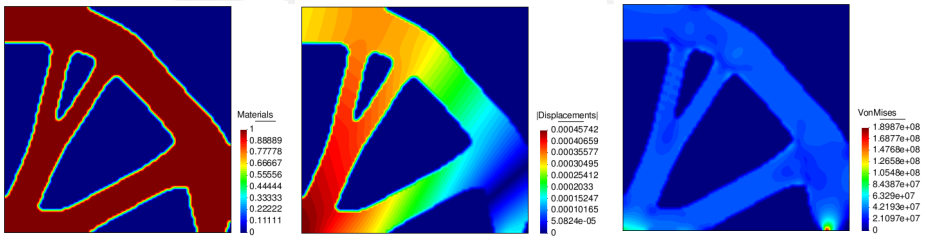

(a) TDLM material (b) TDLM displacements (c) TDLM VonMises

Figure 56: TDLM visual results with SIMP

7.12 MBBB

Data	SIMPSC	SIMPSVC	SIMP
Initial SF	7.4724e-1	-	-
Iterations	174	32	150
Initial Volume	3.0e0	3.0e0	3.0e0
Final Volume	8.7304e-1	1.5e0	3.0e0
Final Volume fraction	2.9101e-1	5.0e-1	5.0e-1
Compliance	7.2730e1	4.1618e1	4.1311e1
X displacement avg	-5.6241e-5	-4.0913e-5	-3.9833e-5
X displacement abs avg	5.6241e-5	4.0913e-5	3.9833e-5
Y displacement avg	-5.0429e-2	-2.8525e-2	-2.8313e-2
Y displacement abs avg	5.0429e-2	2.8525e-2	2.8313e-2
|Displacement|	-2.65497e-3	1.5020e-3	1.4909e-3
Security Factor	9.9933e-1	8.3442e-1	8.4178e-1
Avg(VM/YS)	2.1763e-1	1.1495e-1	1.1495e-1
SD(VM/YS)	3.6821e-2	3.3244e-2	3.3244e-2
Max VonMises	2.1985e8	1.8357e8	1.8519e8

Table 17: MBBB execution data

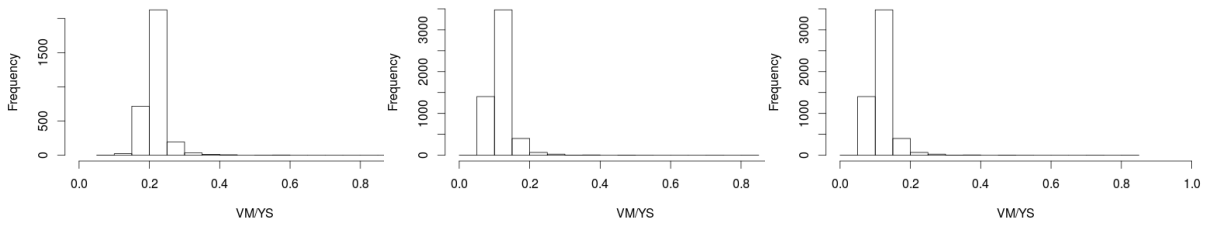

(a) SIMPSC (b) SIMPSVC (c) SIMP

Figure 57: MBBB: VM/YS elemental histogram

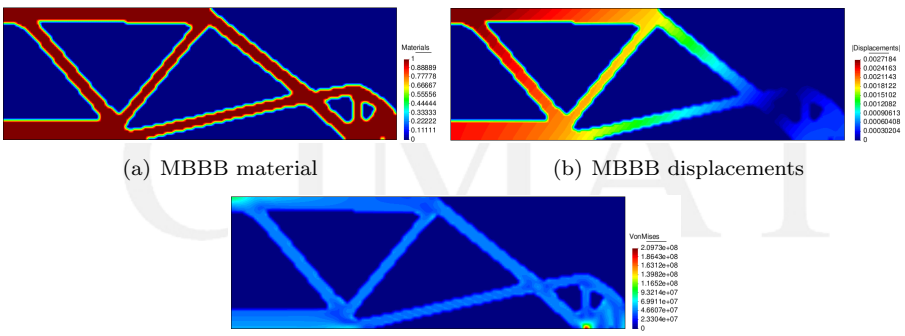

(a) MBBB material (b) MBBB displacements

(c) MBBB VonMises

Figure 58: MBBB visual results with SIMPSC

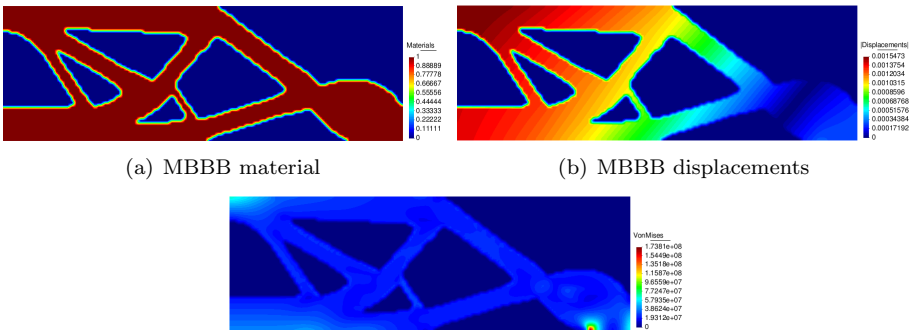

(a) MBBB material (b) MBBB displacements

(c) MBBB VonMises

Figure 59: MBBB visual results with SIMPSVC

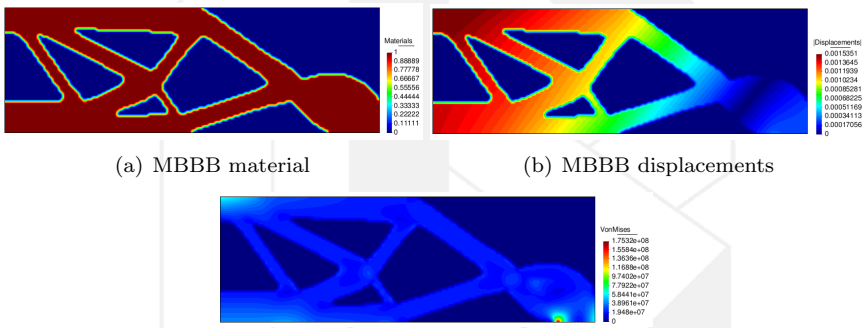

(a) MBBB material (b) MBBB displacements

(c) MBBB VonMises

Figure 60: MBBB visual results with SIMP

7.13 Two Bars

Data	SIMPSC	SIMPSVC	SIMP
Initial SF	7.4920e-1	-	-
Iterations	192	68	96
Initial Volume	2.0e0	2.0e0	2.0e0
Final Volume	2.880e-1	5.0e-1	5.0e-1
Final Volume fraction	1.4404e-1	2.5e-1	2.5e-1
Compliance	1.9446e2	9.8653e1	9.8640e1
X displacement avg	-3.9891e-10	-4.2028e-11	-6.1112e-11
X displacement abs avg	1.0968e-5	4.4010e-6	4.5801e-6
Y displacement avg	-2.1587e-2	-1.0945e-2	-1.0943e-2
Y displacement abs avg	2.1587e-2	1.0945e-2	1.0943e-2
|Displacement|	1.2699e-3	6.4386e-4	6.4378e-4
Security Factor	9.9857e-1	6.1681e-1	6.0319e-1
Avg(VM/YS)	6.8345e-1	3.4487e-1	3.4487e-1
SD(VM/YS)	4.3589e-2	3.0273e-2	2.9974e-2
Max VonMises	2.19686e8	1.3569e8	1.3270e8

Table 18: Two Bars execution data

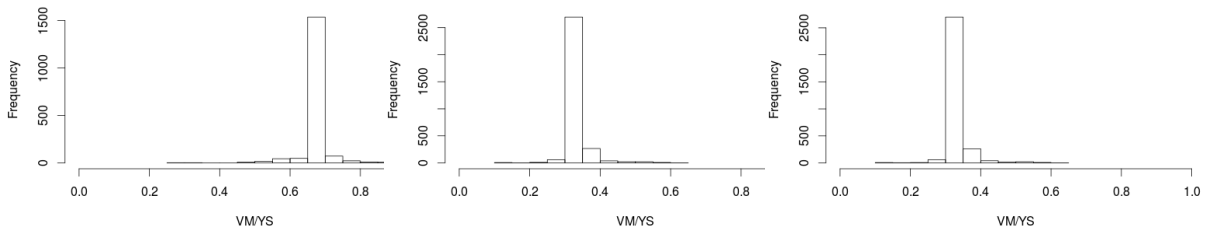

(a) SIMPSC (b) SIMPSVC (c) SIMP

Figure 61: TWO BARS: VM/YS elemental histogram

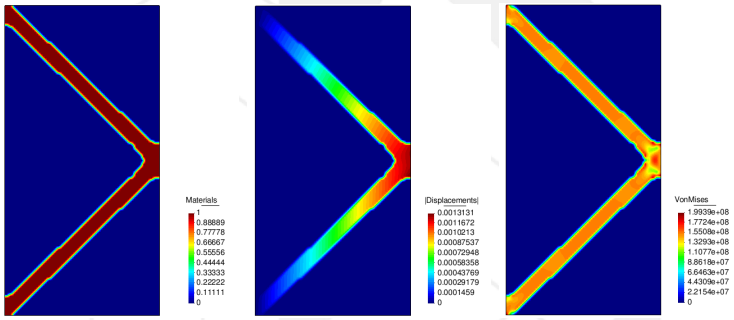

(a) TB material (b) TB displacements (c) TB VonMises

Figure 62: Two Bars visual results with SIMPSC

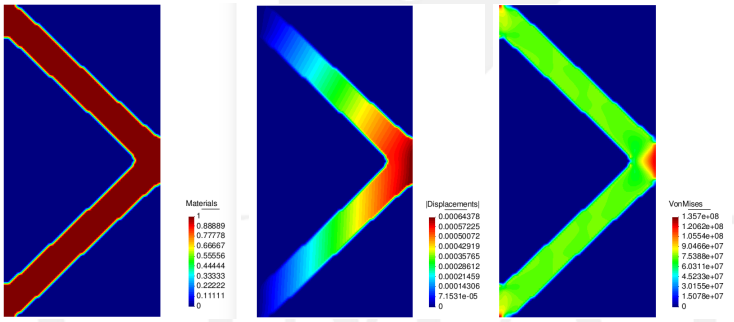

(a) TwoBars material (b) TwoBars displacements (c) TwoBars VonMises

Figure 63: Two Bars visual results with SIMPSVC

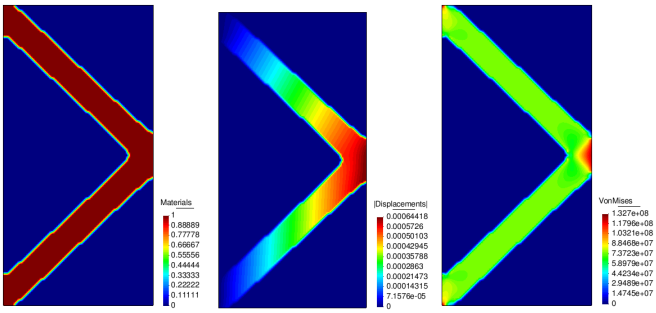

(a) TwoBars material (b) TwoBars displacements (c) TwoBars Von-Mises

Figure 64: Two Bars visual results with SIMP

8 Conclusions

In this report we have introduced a benchmark for topology optimization in 2d, considering plane stress. The purpose of the benchmark is to unify realistic dimensions, material and boundary conditions, in order to perform fair comparisons among competing algorithms. The proposed benchmark can be used under different objective functions, although we present results for two kind of problems: minimize compliance subject to a volume constraint, and minimize volume subject to a stress constraint. In both cases we use variations of the SIMP for reporting approximations to the optimal solutions. Hence, we compare the original SIMP with an improved version which better detects convergence, avoiding to perform excessive evaluations that do not always improve the structure. Furthermore, our improved SIMP version, named SIMPSC, in average uses 77.5% less evaluations than the original SIMP, which was stopped in 150 iterations, because the other recommended stopping criteria are not straight forward tuned for most of the cases. Nevertheless the SIMPSVC significantly uses less evaluations, the compliance difference is in average 0.68 %, what means that the SIMP, actually, does not improve significantly the solution in the last iterations, and often it diminish the quality of the solution. Additionally, we introduce another method called SIMPSC (SIMP with Stress Constraint), which is capable of delivering an approximated solution for the minimum volume problem regarding the maximum permissible von Mises stress. When using the original SIMP one can not have certainty about functionality, because the method does not verify that the structure is working in the elastic range, for example, in the CLC problem reported in Section 7 SIMP and SIMSVC exceed the yield stress while the SIMPSC does not, actually SIMPSC always delivers a structure with security factor around 1.

In summary, the aim of this report is to provide of a benchmark and reference solutions for the 2d topology optimization problem for different objective functions. The resulted benchmark is product of an exhaustive study of literature, and testing of different conditions with one of the best performed algorithms: the original SIMP, and two modified versions.

References

[1] Gregoire Allaire, C. Dapogny, and P. Frey. Shape optimization with a level set based mesh evolution method. *Computer Methods in Applied Mechanics and Engineering*, 282:22–53, 2014.

[2] Gregoire Allaire and Francois Jouve. A level-set method for vibration and multiple loads structural optimization. *Computer Methods in Applied Mechanics and Engineering*, 194:3269–3290, 2005.

[3] Gregoire Allaire, Francois Jouve, and Anca-Maria Toader. A level-set method for shape optimization. *Comptes Rendu Mathematique*, 334:1125–1130, 2002.

[4] Gregoire Allaire, Francois Jouve, and Anca-Maria Toader. Structural optimization using sensitivity analysis and a level-set method. *Journal of Computational Physics*, 194:363–393, 2004.

[5] S. Amstutz, A. A. Novotny, and E. A. de Souza Neto. Topological derivative-based topology optimization of structures subject to drucker-prager stress constraints. *Computer Methods in Applied Mechanics and Engineering*, 233-236:123–136, 2012.

[6] Samuel Amstutz and Heiko Andra. A new algorithm for topology optimization using a level-set method. *Journal of Computational Physics*, 216:573–588, 2006.

[7] Samuel Amstutz and Antonio A Novotny. Topological optimization of structures subject to von mises stress constraints. *Structural and Multidisciplinary Optimization*, 41(3):407–420, 2010.

[8] R. Balamurugan, C.V. Ramakrishnan, and N. Singh. Performance evaluation of a two stage adaptive genetic algorithm (tsaga) in structural topology optimization. *Applied Soft Computing*, 8:1607–1624, 2008.

[9] M. P. Bendsoe and N. Kikuchi. Generating optimal topologies in structural design using a homogenization method. *Computer Methods Applied Mechanics and Engineering*, 71:197–224, 1988.

[10] M. P. Bendsoe and O. Sigmund. Material interpolation schemes in topology optimization. *Archive of Applied Mechanics*, 69:635–654, 1999.

[11] T. Borrvall. Topology optimization of elastic continua using restriction. *Archives of Computational Methods in Engineering*, 8:351–385, 2001.

[12] T. E. Bruns and D. A. Tortorelli. An element removal and reintroduction strategy for the topology optimization of structures and compliant mechanism. *International Journal for Numerical Methods in Engineering*, 57:1413–1430, 2003.

[13] Sujin Bureerat and Jumlong Limtragool. Performance enhancement of evolutionary search for structural topology optimisation. *Finite Elements in Analysis and Design*, 42:547–566, 2006.

[14] Sujin Bureerat and Jumlong Limtragool. Structural topology optimisation using simulated annealing with multiresolution design variables. *Finite Elements in Analysis and Design*, 44:738–747, 2008.

[15] Shouyu Cai and Weihong Zhang. Stress constrained topology optimization with free-form design domains. *Computer Methods in Applied Mechanics and Engineering*, 289:267–290, 2015.

[16] Shouyu Cai, Weihong Zhang, Jihong Zhu, and Tong Gao. Stress constrained shape and topology optimization with fixed mesh: A b-spline finite cell method combined with level-set function. *Computer Methods in Applied Mechanics and Engineering*, 278:361–387, 2014.

[17] Miguel Carrasco, Benjamin Ivorra, and Angel Manuel Ramos. Stochastic topology design optimization for continuous elastic materials. *Computer Methods in Applied Mechanics and Engineering*, 289:131–154, 2015.

[18] R. Cazacu and L. Grama. Overview of structural optimization methods for plane and solid structures. *Annals of the University of Oradea*, 2014.

[19] Jean Cea, Stephane Garreau, Philippe Guillaume, and Mohamed Masmoudi. The shape and topological optimizations connection. *Computer Methods in Applied Mechanics and Engineering*, 188:713–726, 2000.

[20] Bing-Chung Chen and Noboru Kikuchi. Topology optimization with design-dependent loads. *Finite Elements in Analysis and Design*, 37:57–70, 2001.

[21] Shikui Chen, Michael Yu Wang, and Ai Qun Liu. Shape feature control in structural topology optimization. *Computer-Aided Design*, 40:951–962, 2008.

[22] J. D. Deaton and R. V. Grandhi. A survey of structural and multidisciplinary continuum topology optimization: post 2000. *Structural and Multidisciplinary Optimization*, 49:1–38, 2014.

[23] Luca Dede, Micheal J. Borden, and Thomas J. R. Hughes. Isogeometric analysis for topology optimization with a phase field model. *Archives of Computational Methods in Engineering*, 19:427–465, 2012.

[24] H. A. Eschenauer, V. V. Kobelev, and A. Schumacher. Bubble method for topology and shape optimization of structures. *Structural Optimization*, 8:42–51, 1994.

[25] N. P. Garcia-Lopez, M. Sanchez-Silva, A. L. Medaglia, and A. Chateauneuf. An improved robust topology optimization approach using multiobjective evolutionary algorithms. *Computers and Structures*, 125:1–10, 2013.

[26] James K. Guest and Lindsey C. Smith Genut. Reducing dimensionality in topology optimization using adaptive design variable fields. *International Journal for Numerical Methods in Engineering*, 81:1019–1045, 2010.

[27] Xu Guo, Wei Sheng Zhang, Michael Yu Wang, and Peng Wei. Stress-related topology optimization via level set approach. *Computer Methods in Applied Mechanics and Engineering*, 200:3439–3452, 2011.

[28] Xu Guo, Weisheng Zhang, and Li Zhang. Robust structural topology optimization considering boundary uncertainties. *Computer Methods in Applied Mechanics and Engineering*, 253:356–368, 2013.

[29] Xu Guo, Weisheng Zhang, and Whenliang Zhong. Explicit feature control in structural topology optimization via level set method. *Computer Methods in Applied Mechanics and Engineering*, 272:354–378, 2014.

[30] Wilfried Hansel, Andre Treptow, Wilfried Becker, and Bernd Freisleben. A heuristic and a genetic topology optimization algorithm for weight-minimal laminate structures. *Composite Structures*, 58:287–294, 2002.

[31] X. Huang and Y. M. Xie. Evolutionary topology optimization of continuum structures with an additional displacement constraint. *Structural and Multidisciplinary Optimization*, 40:409–416, 2010.

[32] Kai A. James, Edmund Lee, and Joaquim R.R.A. Martins. Stress-based topology optimization using an isoparametric level set method. *Finite Elements in Analysis and Design*, 58:20–30, 2012.

[33] Seung Hyun Jeong, Dong-Hoon Choi, and Gil Ho Yoon. Separable stress interpolation scheme for stress-based topology optimization with multiple homogenous materials. *Finite Elements in Analysis and Design*, 82:16–31, 2014.

[34] Seung Hyun Jeong, Gil Ho Yoon, Akihiro Takezawa, and Dong-Hoon Choi. Development of a novel phase-field method for local stress-based shape and topology optimization. *Computers and Structures*, 132:84–98, 2014.

[35] Helio Emmendoerfer Jr. and Eduardo Alberto Fancello. A level set approach for topology optimization with local stress constraints. *International Journal for Numerical Methods in Engineering*, 99:129–156, 2014.

[36] Zhan Kang and Yiqiang Wang. A nodal variable method of structural topology optimization based on shepard interpolant. *International Journal for Numerical Methods in Engineering*, 90:329–342, 2012.

[37] Zhan Kang and Yiqiang Wang. Integrated topology optimization with embedded movable holes based on combined description by material density and level sets. *Computer Methods in Applied Mechanics and Engineering*, 255:1–13, 2013.

[38] Zhang Kang and Yiqiang Wang. Structural topology optimization based on non-local shepard interpolation of density field. *Computer Methods in Applied Mechanics and Engineering*, 200:3515–3525, 2011.

[39] Sun Yong Kim, Il Yong Kim, and Chris K. Mechefske. A new efficient convergence criterion for reducing computational expense in topology optimization: reducible design varialbe method. *International Journal for Numerical Methods in Engineering*, 90:752–783, 2012.

[40] M. Akif Kutuk and Ibrahim Gov. A finite element removal method for 3d topology optimization. *Advances in Mechanical Engineering*, 2013(413463), 2013.

[41] Euihark Lee and Hae Chang Gea. A strain based topology optimization method for compliant mechanism design. *Structural and Multidisciplinary Optimization*, 49:199–207, 2014.

[42] T. Lewinski and G.I.N. Rozvany. Exact analytical solutions for some popular benchmark problems in topology optimization ii: thress-sided polygonal supports. *Structural and Multidisciplinary Optimization*, 33:337–349, 2007.

[43] T. Lewinski and G.I.N. Rozvany. Analytical benchmark for topological optimization iv: square-shaped line support. *Structural and Multidisciplinary Optimization*, 36:143–158, 2008.

[44] T. Lewinski, G.I.N. Rozvany, T. Sokol, and K. Bolbotowski. Exact analytical solutions for some popular benchmark problems in topology optimization iii: L-shaped domains revisited. *Structural and Multidisciplinary Optimization*, 47:937–942, 2013.

[45] Guan-Chun Luh, L. Chun-Yi, and L. Yu-Shu. A binary particle swarm optimization for continuum structural topology optimization. *Applied Soft Computing*, 11(2):2833–2844, 2011.

[46] Guan-Chun Luh and Chun-Yi Lin. Structural topology optimization using ant colony optimization algorithm. *Applied Soft Computing*, 9:1343–1353, 2009.

[47] Junzhao Luo, Zhen Luo, Liping Chen, Liyong Tong, and Michael Yu Wang. A semi-implicit level set method for structural shape and topology optimization. *Journal of Computational Physics*, 227:5561–5581, 2008.

[48] Yangjun Luo and Zhan Kang. Topology optimization of continuum structures with drucker-prager yield. *Computers and Structures*, 90-91:65–75, 2012.

[49] Yangjun Luo, Michael Yu Wang, and Zhan Kang. An enhanced aggregation method for topology optimization with local stress constraints. *Computer Methods in Applied Mechanics and Engineering*, 254:31–41, 2013.

[50] Z. Luo, N. Zhang, W. Gao, and H. Ma. Structural shape and topology optimization using a meshless galerkin level set method. *International Journal for Numerical Methods in Engineering*, 90:369–389, 2012.

[51] Zhen Luo and Liyong Tong. A level set method for shape and topology optimization of large-displacement compliant mechanisms. *International Journal for Numerical Methods in Engineering*, 76:862–892, 2008.

[52] Zhen Luo, Liyong Tong, and Zhang Kang. A level set method for structural shape and topology optimization using radial basis functions. *Computers and Structures*, 87:425–434, 2009.

[53] Zhen Luo, Michael Yu Wang, Shengyin Wang, and Peng Wei. A level set-based parameterization method for structural shape and topology optimization. *International Journal for Numerical Methods in Engineering*, 76:1–26, 2008.

[54] K. Matsui and K. Terada. Continuous approximation of material distribution for topology optimization. *International Journal for Numerical Methods in Engineering*, 59:1925–1944, 2004.

[55] P. B. Nakshatrala, D. A. Tortorelli, and K. B. Nakshatrala. Nonlinear structural desing using multiscale topology optimization. *Computer Methods in Applied Mechanics and Engineering*, 261-252:167–176, 2013.

[56] Luis Carretero Neches and Adrián P. Cisilino. Topology optimization of 2d elastic structures using boundary elements. *Engineering Analysis with Boundary Elements*, 32:533–544, 2008.

[57] Tam H. Nguyen, Glaucio H. Paulino, Junho Song, and Chau H. Le. Improving multiresolution topology optimization via multiple discretizations. *International Journal for Numerical Methods in Engineering*, 92:507–530, 2012.

[58] Norapat Noilublao and Sujin Bureerat. Simultaneous topology, shape, and sizing optimisation of plane trusses with adaptive ground finite elements using moeas. *Mathematical Problems in Engineering*, 2013, 2013.

[59] M. Papadrakakis, N. D. Lagaros, Y. Tsompanakis, and V. Plevris. Large scale structural optimization: Computational methods and optimization algorithms. *Archives of Computational Methods in Engineering*, 3:239–301, 2001.

[60] J. Paris, I. Colominas, F. Navarrina, and M. Casteleiro. Parallel computing in topology optimization of structures with stress constraints. *Computers and Structures*, 125:62–73, 2013.

[61] Jaejong Park and Alok Sutradhar. A multi-resolution method for 3d multi-material topology optimization. *Computer Methods in Applied Mechanics and Engineering*, 285:571–586, 2015.

[62] Xiaoping Qian. Topology optimization in b-spline space. *Computer Methods in Applied Mechanics and Engineering*, 265:15–35, 2013.

[63] Osvaldo Maximo Querin, Mariano Victoria, and Pascual Marti. Topology optimization of truss-like continua with different material properties in tension and compression. *Structural and Multidisciplinary Optimization*, 42:25–32, 2010.

[64] Stefan Riehl and Paul Steinmann. A staggered approach to shape and topology optimization using the traction method and an evolutionary-type advancing front. *Computer Methods in Applied Mechanics and Engineering*, 287:1–30, 2015.

[65] Jian Hua Rong, Xiao Hua Liu, Ji Jun Yi, and Jue Hong Yi. An efficient structural topological optimization method for continuum structures with multiple displacement constraints. *Finite Elements in Analysis and Design*, 47:913–921, 2011.

[66] G.I.N. Rozvany. Exact analytical solutions for some popular benchmark problems in topology optimization. *Structural Optimization*, 15:42–48, 1998.

[67] Hyunjin Shin, Akira Todoroki, and Yoshiyasu Hirano. Elite-initial population for efficient topology optimization using multi-objective genetic algorithms. *International Journal of Aeronautical & Space Sciences*, 14:324–333, 2013.

[68] O. Sigmund. A 99 line topology optimization code written in matlab. *Structural and Multidisciplinary Optimization*, 21:120–127, 2001.

[69] M. Stolpe and K. Svanberg. An alternative interpolation scheme for minimum compliance topology optimization. *Structural and Multidisciplinary Optimization*, 22:116–124, 2001.

[70] K. Svanberg and M. Werme. Topology optimization by a neighbourhood search method based on efficient sensitivity calculations. *International Journal for Numerical Methods in Engineering*, 67:1670–1699, 2006.

[71] Colby C. Swan and Iku Kosaka. Voigt-reuss topology optimization structures with linear elastic material behaviours. *International Journal for Numerical Methods in Engineering*, 40:3033–3057, 1997.

[72] Akihiro Takezawa, Gil Ho Yoon, Seung Hyun Jeong, Makoto Kobashi, and Mitsuru Kitamura. Structural topology optimization with strength and heat conduction constraints. *Computer Methods in Applied Mechanics and Engineering*, 276:341–361, 2014.

[73] Cameron Talischi, Glaucio H. Paulino, Anderson Pereira, and Ivan F. M. Menezes. Polygonal finite elements for topology optimization: A unifying paradigm. *International Journal for Numerical Methods in Engineering*, 82:671–698, 2010.

[74] Rouhollah Tavakoli. Multimaterial topology optimization by volume constrained allen-cahn system and regularized projected steepest descent method. *Computer Methods in Applied Mechanics and Engineering*, 276:534–565, 2014.

[75] Liyong Tong and Jiangzi Lin. Structural topology optimization with implicit design variable-optimality and algorithm. *Finite Elements in Analysis and Design*, 47:922–932, 2011.

[76] B. Ullah and J. Trevelyan. Correlation between hole insertion criteria in a boundary element and level set based topology optimisation method. *Engineering Analysis with Boundary Elements*, 37:1457–1470, 2013.

[77] N. P. van Dijk, M. Langelaar, and F. van Keulen. Explicit level-set-based topology optimization using an exact heaviside function and consistent sensitivity analysis. *International Journal for Numerical Methods in Engineering*, 91:67–97, 2012.

[78] Mathias Wallin and Matti Ristinmaa. Howard's algorithm in a phase-field topology optimization approach. *International Journal for Numerical Methods in Engineering*, 94:43–59, 2013.

[79] Mathias Wallin and Matti Ristinmaa. Boundary effects in a phase-field approach to topology optimization. *Computer Methods in Applied Mechanics and Engineering*, 278:145–159, 2014.

[80] Mathias Wallin and Matti Ristinmaa. Topology optimization utilizing inverse motion based form finding. *Computer Methods in Applied Mechanics and Engineering*, 289:316–331, 2015.

[81] Fengwen Wang, Boyan Stefanov Lazarov, Ole Sigmund, and Jakob Sondergaard Jasen. Interpolation scheme for fictitious domain techniques and topology optimization of finite strain elastic problems. *Computer Methods in Applied Mechanics and Engineering*, 276:453–472, 2014.

[82] Michael Yu Wang and Shengyin Wang. Bilateral filtering for structural topology optimization. *International Journal for Numerical Methods in Engineering*, 63:1911–1938, 2005.

[83] Michael Yu Wang and Xiaoming Wang. "color" level sets: a multiphase method for structural topology optimization with multiple materials. *Computer Methods in Applied Mechanics and Engineering*, 193:469–496, 2004.

[84] Michael Yu Wang and Xiaoming Wang. A level-set based variational method for design and optimization of heterogeneous objects. *Computer-Aided Design*, 37:321–337, 2005.

[85] Michael Yu Wang, Xiaoming Wang, and Dongming Guo. A level set method for structural topology optimization. *Computer Methods in Applied Mechanics and Engineering*, 192:227–246, 2003.

[86] S. Y. Wang, K. M. Lim, B. C. Khoo, and M. Y. Wang. An extended level set method for shape and topology optimization. *Journal of Computational Physics*, 221:395–421, 2007.

[87] S. Y. Wang and M. Y. Wang. An enhanced genetic algorithm for structural topology optimization. *International Journal for Numerical Methods in Engineering*, 65:18–44, 2006.

[88] Yiqiang Wang, Zhan Kang, and Qizhi He. Adaptive topology optimization with independent error control for separated displacement and density fields. *Computers and Structures*, 135:50–61, 2014.

[89] Yiqiang Wang, Zhen Luo, Zhan Kang, and Nong Zhang. A multi-material level set-based topology and shape optimization method. *Computer Methods in Applied Mechanics and Engineering*, 283:1570–1586, 2015.

[90] Liang Xia and Piotr Breitkopf. Concurrent topology optimization design of material and structure within fe^2 nonlinear multiscale analysis framework. *Computer Methods in Applied Mechanics and Engineering*, 278:524–542, 2014.

[91] Liang Xia and Piotr Breitkopf. A reduced multiscale model for nonlinear structural topology optimization. *Computer Methods in Applied Mechanics and Engineering*, 280:117–134, 2014.

[92] Liang Xia and Piotr Breitkopf. Multiscale structural topology optimization with an approximate constitutive model for local material microstructure. *Computer Methods in Applied Mechanics and Engineering*, 286:147–167, 2015.

[93] Liang Xia, Jihong Zhu, Weihong Zhang, and Piotr Breitkopf. An implicit model for the integrated optimization of component layout and structure topology. *Computer Methods in Applied Mechanics and Engineering*, 257:87–102, 2013.

[94] Qi Xia, Tielin Shi, Shiyuan Liu, and Michael Yu Wang. A level set solution to the stress-based structural shape and topology optimization. *Computers and Structures*, 90-91:55–64, 2012.

[95] Qi Xia, Michael Yu Wang, and Tielin Shi. A level set method for shape and topology optimization of both structure and support of continuum structures. *Computer Methods in Applied Mechanics and Engineering*, 272:340–353, 2014.

[96] Qi Xia, Michael Yu Wang, and Tielin Shi. Topology optimization with pressure load through a level set method. *Computer Methods in Applied Mechanics and Engineering*, 283:177–195, 2015.

[97] Qi Xia and Yu Wang. Simultaneous optimization of the materials properties and the topology of functionally graded structures. *Computer-Aided Design*, 40:660–675, 2008.

[98] Huayang Xu, Liwen Guan, Xiang Chen, and Liping Wang. Guide-weight motion for topology optimization of continuum structures including body forces. *Finite Elements in Analysis and Design*, 75:38–49, 2013.

[99] Shintaro Yamasaki, Atsushi Kawamoto, Tsuyoshi Nomura, and Kikuo Fujita. A consistent grayscale-free topology optimization method using the level-set method and zero-level boundary tracking mesh. *International Journal for Numerical Methods in Engineering*, 101:744–773, 2015.

[100] Shintaro Yamasaki, Shinji Nishiwaki, Takayuki Yamada, Kazuhiro Izui, and Masataka Yoshimura. A structural optimization method based on the level set method using a new geometry-based re-initialization scheme. *International Journal for Numerical Methods in Engineering*, 83:1580–1624, 2010.

[101] Tong Yifei, Ye Wei, Yang Zhen, Li Dongbo, and Li Xiangdong. Research on multidisciplinary optimization design of bridge crane. *Mathematical Problems in Engineering*, 2013, 2013.

[102] Mei Yulin and Wang Xiaoming. A level set method for structural topology optimization and its applications. *Advances in Engineering Software*, 35:415–441, 2004.

[103] Weisheng Zhang, Wenliang Zhong, and Xu Guo. An explicit length scale control approach in simp-based topology optimization. *Computer Methods in Applied Mechanics and Engineering*, 282:71–86, 2014.

[104] Hongwei Zhao, Kai Long, and Z. D. Ma. Homogenization topology optimization method based on continuous field. *Advances in Mechanical Engineering*, 2010(528397), 2010.

[105] Junpeng Zhao and Chunjie Wang. Robust topology optimization under loading uncertainty based on linear elastic theory and orthogonal diagonalization of symmetric matrices. *Computer Methods in Applied Mechanics and Engineering*, 272:204–218, 2014.

[106] Benliang Zhu, Xianmin Zhang, and Sergej Fatikow. Structural topology and shape optimization using a level set method with distance-suppression scheme. *Computer Methods in Applied Mechanics and Engineering*, 283:1214–1239, 2015.

[107] Ji-Hong Zhu, Wei-Hong Zhang, and Liang Xia. Topology optimization in aircraft and aerospace structures. *Archives of Computational Methods in Engineering*, 2015.